Molecular Therapy
Oncolytics
Original Article

Preclinical evaluation of a novel antibody-drug conjugate targeting DR5 for lymphoblastic leukemia therapy

Shuyong Zhang,[1,2] Dongdong Zhou,[1] Chao Zheng,[1] Peng Xiong,[1] Wan Zhu,[1] and Dexian Zheng[1,2]

[1]Yantai Obioadc Biomedical Technology Ltd., Yantai, China; [2]Obio Technology (Shanghai) Corp, Ltd., No. 908, Building 19, Ziping Road, Pudong New District, Shanghai 201321, China

Acute lymphoblastic leukemia (ALL) is an aggressive hematological neoplasm resulting from immature lymphoid precursors. An antibody-drug conjugate (ADC), coupling a small molecule covalently with a targeting antibody, can specifically kill tumor cells. Death receptor 5 (DR5) is considered as a promising anti-tumor drug target. In this study, we describe the preclinical evaluation of a novel DR5-targeting ADC (Oba01) as a potential therapeutic against ALL. Oba01 utilizes anti-DR5 humanized monoclonal antibody (zaptuzumab) coupled via a cleavable linker to monomethyl auristatin E (MMAE). Oba01 can specifically bind to DR5 on the tumor cells and transfer into lysosome via DR5-mediated endocytosis. It then effectively releases the MMAE, which can bind to the tubulin and prevent its aggregation, thereby leading to a significant inhibition of proliferation and cell death in tumor cells. Additionally, Oba01 displays significant dose-dependent tumoricidal activity in cell-derived xenograft (CDX) and patient-derived xenograft (PDX) mouse models. More importantly, toxicity analysis of Oba01 showed a favorable safety profile, and pharmacokinetic analysis illustrated an excellent stability and tolerability in rats and cynomolgus monkeys. Taken together, our data conclusively demonstrate that Oba01 is an attractive candidate for further clinical trials in DR5-positive ALL patients.

INTRODUCTION

Acute lymphoblastic leukemia (ALL) is an aggressive hematological neoplasm resulting from abnormal proliferation of immature lymphoid precursors. ALL is more common in children, with a high incidence rate in the age group of 2–4 years. The current complete remission rate is more than 90%, and the disease-free survival rate is 70%–80%. In adults, 75% of ALL cases develop from B cell precursors and the remainder from T cell precursors.[1–6] However, the prognosis of ALL remains poor, and hence development of novel therapeutics to improve the treatment outcome is urgently needed.

Therapeutic antibodies are being actively used in clinical settings as the standard of care for the management of various solid tumors and hematological malignancies. Moreover, targeting antibody-drug conjugates (ADCs) could specifically bind to the tumor-related antigen on the cell surface, and then could be endocytosed into lysosomes, where the payload of a small-molecule toxin coupled to the antibody could be effectively released by proteinase digestion and specifically kill the tumor cells.[7–11] Thus, ADCs have become an important strategy in development of the novel cancer therapeutics. As of now, several ADCs have been approved by the US Food and Drug Administration (FDA) or European Medicines Agency (EMA), for example, gemtuzumab ozogamicin (Mylotarg, Pfizer) for the treatment of CD33-expressing acute myelogenous leukemia,[12] brentuximab vedotin (Adcetris, Seattle Genetics) for the therapy of CD30-positive Hodgkin's lymphoma,[13] ado-trastuzumab-emtansine (Kadcyla, Genentech) for the treatment of Her2-positive breast cancer,[14] inotuzumab ozogamicin (Besponsa, Pfizer) for the management of CD22-expressing relapsed and refractory B cells and ALL,[15] polatuzumab vedotin (Polivy, Roche) for the therapy of CD79B-expressing relapsed and refractory diffuse large B cell lymphoma (R/R DLBCL),[16] trastuzumab deruxtecan (Enhertu, AstraZeneca/Daiichi Sankyo) for the treatment of Her2-positive breast cancer,[17] and enfortumab vedotin (Padcev, Seattle Genetics/Astellas) for the therapy of Nectin-4-positive bladder cancer.[18] Currently, more than 10 ADCs are undergoing phase III clinical trials in cancer patients.[11] However, there remains an unmet need to a great extent for the development of effective therapeutics against various malignant tumors, including ALL.

Tumor necrosis factor-related apoptosis-inducing ligand (TRAIL) receptor 2 (TRAIL-R2/CD262), also known as death receptor 5 (DR5), is a type I membrane molecule belonging to the tumor necrosis factor receptor superfamily.[19,20] DR5 is highly expressed in the various cancers, such as lymphocytic leukemia, lung carcinoma, pancreatic cancer, colon cancer, breast cancer, ovarian cancer, and bladder cancer, among others, but it is minimally expressed in most of the normal cells.[21–23] DR5 has been considered as a promising and potential therapeutic target for the development of anticancer agents. Interestingly, various cancer therapies targeting DR5, including the recombinant soluble TRAIL (rsTRAIL) or anti-DR5 agonistic monoclonal antibodies,

Received 18 November 2020; accepted 25 April 2021;
https://doi.org/10.1016/j.omto.2021.04.013.

Correspondence: Dexian Zheng, Obio Technology (Shanghai) Corp., Ltd., No. 908, Building 19, Ziping Road, Pudong New District, Shanghai 201321, China.
E-mail: zhengdx@pumc.edu.cn

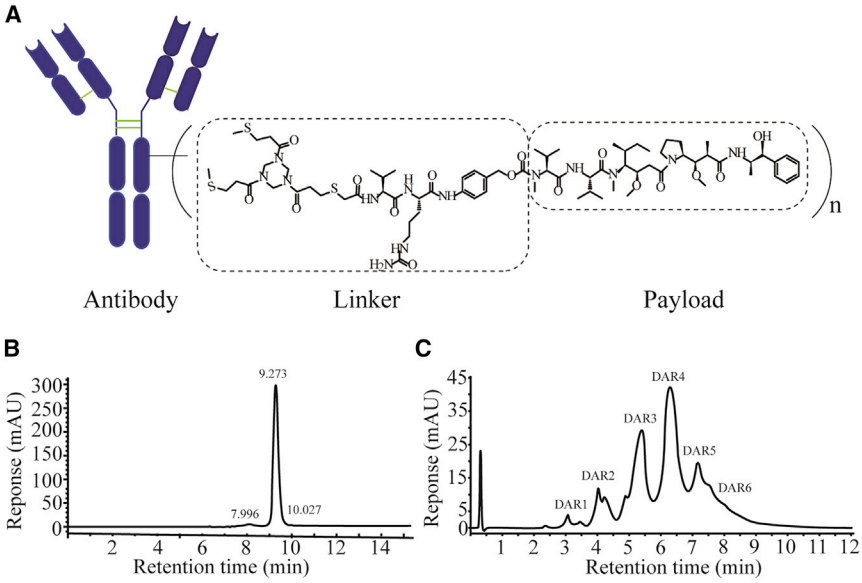

Figure 1. Characterization of Oba01

(A) The structure of Oba01. (B) Oba01 as characterized by size-exclusion chromatography. (C) Hydrophobic interaction chromatography depicting different drug/antibody ratio (DAR) isoforms of Oba01.

have been tested in the phase I/II clinical trials for multiple tumors.[24,25] In a previous study, we first reported that a novel highly potent first-in-class ADC named Zapadcine-1 can effectively target DR5 and displays an excellent antitumor activity against both solid tumors and hematological malignancies, but the therapeutic window of this ADC was markedly lower for effective human cancer therapy.[26]

In the present study, we report a comprehensive preclinical evaluation of another novel DR5-targeting ADC (designated as Oba01) for the potential use in DR5-positive ALL therapy. Oba01 utilizes the humanized DR5-specific monoclonal antibody zaptuzumab coupled via a cleavable linker to a highly toxic inhibitor of tubulin, monomethyl auristatin E (MMAE), by using ThioBridge technology.[26,27] We explored its possible anti-tumor efficacy in both *in vitro* and *in vivo* models. The toxicity and pharmacokinetic (PK) analysis of Oba01 demonstrated excellent safety, stability, and tolerability in both Sprague-Dawley (SD) rats and cynomolgus monkeys, indicating that Oba01 can potentially act as an attractive therapeutic candidate for further clinical investigation in patients with DR5-positive ALL.

RESULTS

Generation of DR5-targeting ADC Oba01

Oba01 is an ADC composed of zaptuzumab, a humanized anti-DR5 antibody (immunoglobulin [Ig]G1), coupled with a cleavable valine-citrulline-dipeptide linker (PY-MAA-Val-Cit-PAB) and a highly potent microtubule-disrupting toxin, MMAE, by using ThioBridge technology.[26,27] (Figure 1A). The ADC was 97.05% monodispersed as determined by size-exclusion chromatography (SEC) (Figure 1B; Table S2). The drug/antibody ratio (DAR) determined by hydrophobic interaction chromatography (HIC) was 4.0 (Figure 1C; Table S3). Additionally, the binding selectivity of Oba01 was also characterized by comparing its interactions with the extracellular domain (ECD) of DR5 from mice, SD rats, cynomolgus monkeys, and human subjects, indicating that half-maximal effective concentrations (EC_{50}s) of Oba01 were 1.262, 0.4171, 0.2099, and 0.01683 nM, respectively (Figure S1). These data suggest that SD rats and cynomolgus monkeys are relevant animal species for the follow-up toxicology assessment of the Oba01 ADC before the clinical applications.

Selective cytotoxicity of Oba01 in ALL cell lines

To investigate the cytotoxicity of Oba01, we first explored the binding ability of Oba01 with various ALL cell lines by using flow cytometry (FCM). It is shown that Oba01 could effectively bind to Jurkat E6-1, Jurkat, A3, J.gamma1, Reh, and MT-4 cells, but not to TF-1, Kasumi-1, and Daudi cells (Figure S2), thereby suggesting that Jurkat E6-1, Jurkat, A3, J.gamma1, Reh, and MT-4 cells can express significantly higher levels of DR5. The cytotoxicity of Oba01 was evaluated in the panel of human lymphoblastic leukemia cells by CellTiter-Glo luminescent cell viability assay. As shown in Figure 2A, Oba01 demonstrated significant cytotoxicity against Jurkat E6-1, Jurkat, J.gamma1, Reh, A3, and MT-4 cells with 50% inhibitory concentration (IC_{50}) values of 7.927, 7.855, 3.141, 0.03766, 2.034, and 6.578 nM, respectively, but it exhibited its cytotoxic action at a concentration >100 μM in TF-1, Kasumi-1, and Daudi cells. In contrast, MMAE was observed to be cytotoxic toward all of the ALL lines tested, and no discrimination was observed between DR5-positive and DR5-negative cells. Additionally, the non-conjugated antibody zaptuzumab also exhibited cytotoxicity toward DR5-positive ALL cell lines. However, the non-targeted ADC, anti-HER-2 ADC of hertuzumab-MC-VC-PAB-MMAE, was found to be insensitive toward both DR5-positive and DR5-negative cell lines.

ADC internalization is one of the key requirements to facilitate its druggability.[11] As demonstrated in Figure 3A, Oba01 induced a significant time-dependent decrease in the expression of cell-surface DR5. In addition, Oba01 (green) was visible on the cells at 4°C and could be distinguished from lysosome-specific LAMP-1 that stained the lysosomes (red) in the cells (Figure 3B). After incubation at 37°C for 30 min, Oba01 was observed to be gradually internalized and visible inside of the cells, where it was found to be co-localized with LAMP-1 in the cytotoxicity of the lysosomes (Figure 3B), thereby indicating that Oba01 could bring the payload into the lysosomes through facilitating internalization.

To assess the possible apoptotic actions of Oba01 on Reh and TF-1 cells, FCM was used to detect annexin V/propidium iodide (PI)-positive cells.

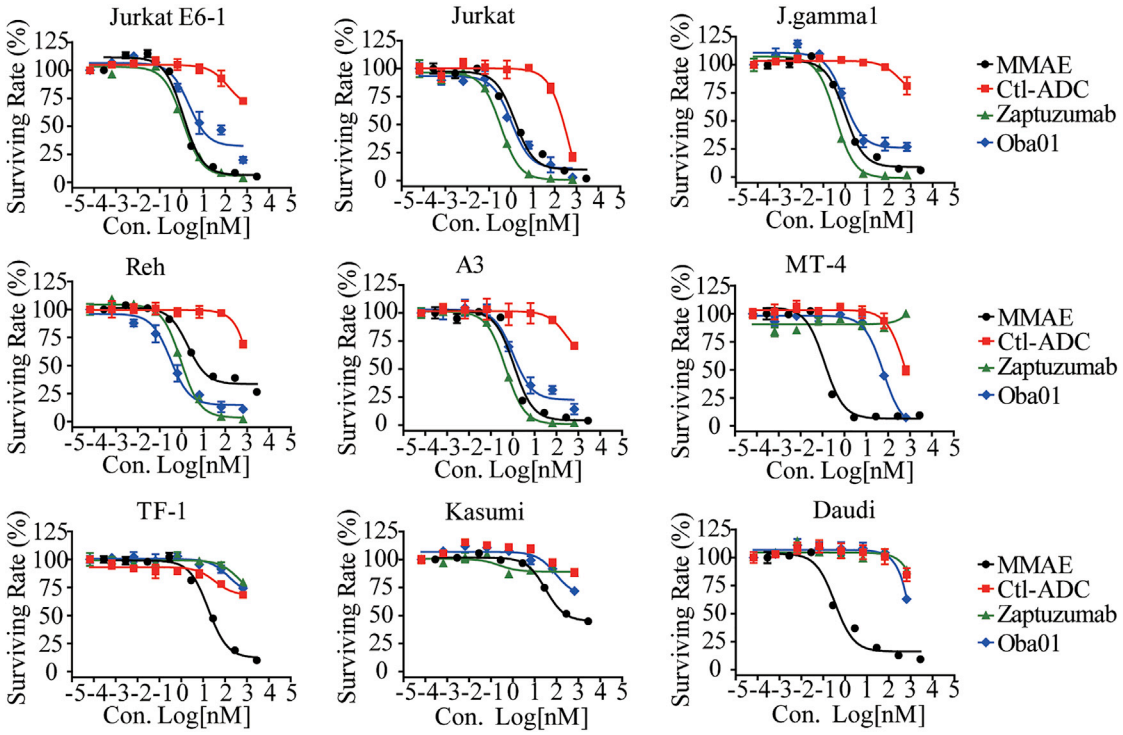

Figure 2. Selective cytotoxicity of Oba01 under *in vitro* conditions

Jurkat E6-1, Jurkat, J.gamma1, Reh, A3, MT-4, TF-1, Kasumi-1, and Daudi cells were treated with increasing concentrations of Oba01, zaptuzumab, MMAE, and hertuzumab-MC-VC-PAB-MMAE (Ctl-ADC) for 72 h. Thereafter, the cell growth and viability were determined by a CellTiter-Glo luminescent cell viability assay according to the manufacturer's instructions.

As shown in Figure 3C, there was a substantial increase of annexin V/PI-positive cells in a dose-dependent manner in DR5-positive Reh cells after Oba01 treatment for 48 h. However, Oba01 did not induce substantial apoptosis in DR5-negative TF-1 cells (Figure 3D). Caspase-3/8 activation is considered as a key biomarker of apoptosis.[28,29] As illustrated in Figure 3E, Oba01 caused a significant upregulation of caspase-3 activity and promoted a moderate increase in caspase-8 activity in the cellular lysate of Reh cells. Collectively, our results suggested that Oba01 could induce significant apoptosis in DR5-positive ALL cells.

In vivo efficacy of Oba01

Subsequently, the potential effects of Oba01 on the growth of human tumor xenografts in mice were evaluated. First, BALB/c nude mice bearing subcutaneous Reh ALL xenografts were administrated Oba01 intravenously (i.v.) via tail vein once every three days for three times (Q3D × 3), and the tumor growth was observed for 67 days. As shown in Figure S3A, Oba01 induced a significant tumor regression at the dosages of 3 and 9 mg/kg. Complete tumor regression (CR) on day 67 was observed in one of seven animals in the 1 mg/kg oba01 dose group, four of seven animals in the 3 mg/kg dose group, and six of seven animals in the 9 mg/kg dose group. Thereafter, the tumor-bearing mice were administered Oba01 intravenously via tail vein once every week for four times (Q1W × 4) and the tumor size was observed for 35 days. As shown in Figure S3C, Oba01 displayed an impressive and significant anti-tumor activity in a dose-dependent manner. The CR was noted in six of eight animals in the 3 mg/kg group on day 35, and in eight of eight animals in the 9 mg/kg group on day 35. Meanwhile, the tumor-bearing mice were intravenously administered Oba01 via tail vein once every two weeks for three times (Q2W × 3) and the tumor sizes were monitored for 43 days. As shown in Figure S3E, Oba01 induced substantial tumor regression at doses of 4 and 8 mg/kg, and the CR was seen in four of six animals in the 8 mg/kg group on day 43. Moreover, no notable body weight changes were observed in all animals during the experimental process (Figures S3B, S3D, and S3F).

We further tested the efficacy of a single intravenously administered dose in Reh xenografts. As shown in Figures 4A, 4B, and S4A, Oba01 elicited tumor regression followed by a marked delay in tumor progression. The CR was seen in nine of nine animals in the 8 mg/kg group on day 12, and this group remained free of palpable tumors until day 21, when the experiment was ended. The CR was also observed in two of nine animals in the 2 mg/kg group and one of nine animals in the 4 mg/kg group on day 21. However, the free form of MMAE (0.08 mg/kg, an equal mole of MMAE in the dosage of Oba01 of 4 mg/kg) exhibited no significant inhibitory effect on the tumor growth. The non-conjugated antibody zaptuzumab (8 mg/kg) also showed a significant suppression of the tumor growth in the mouse xenograft model, but it was comparable to Oba01 of 2 mg/kg, thereby

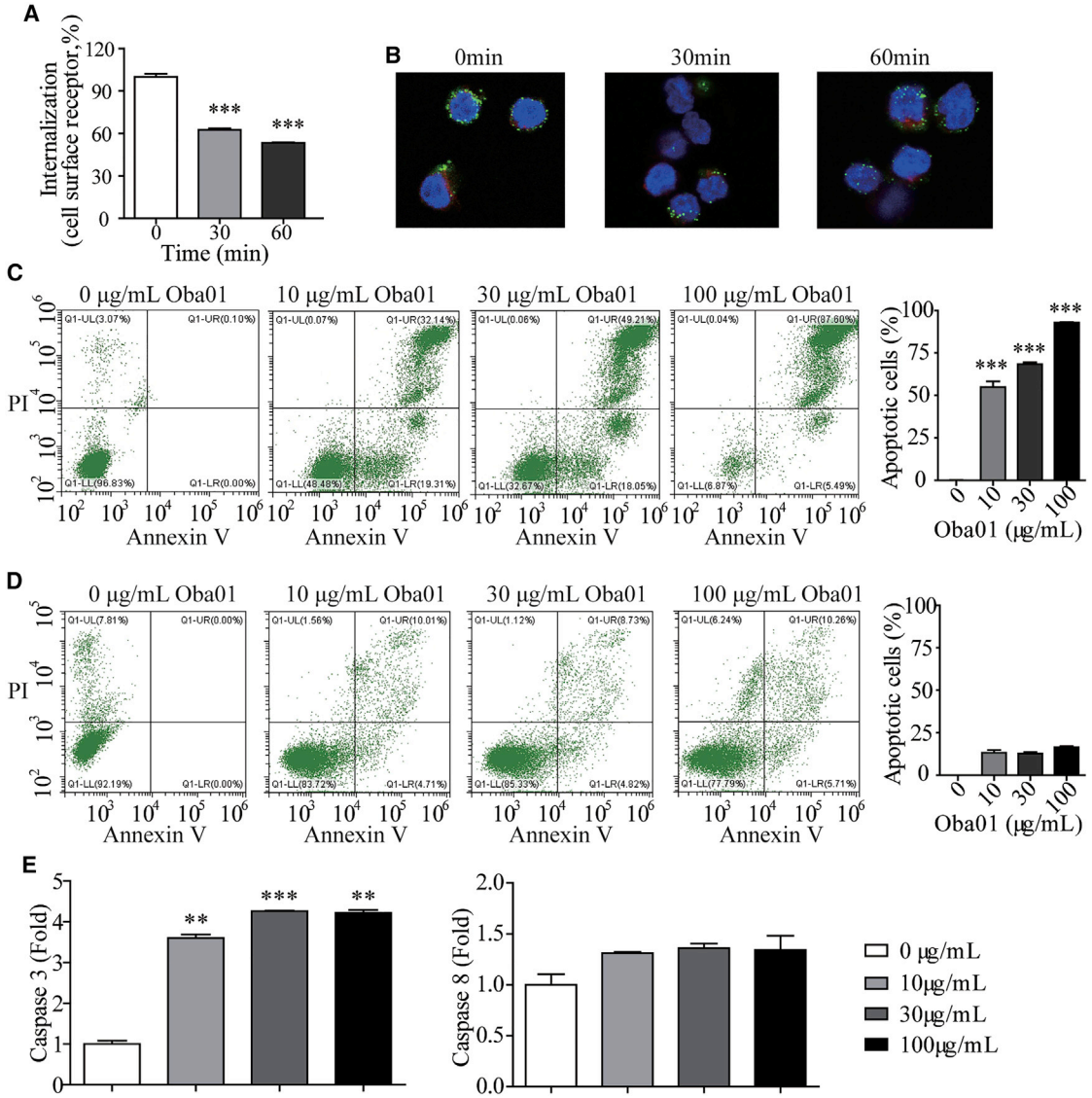

Figure 3. Oba01 induces endocytosis, apoptosis, and caspase-3/8 activation in lymphoblastic leukemia cells

(A) DR5 expression was detected on the Reh cell surface by flow cytometric analysis. (B) Internalization and lysosomal localization of Oba01 in Reh cells by a laser scanning confocal microscope. (C and D) Reh (C) and TF-1 (D) cells were incubated with Oba01 for 2 days, and then cell death was detected by using an annexin V-FITC/PI apoptosis kit by flow cytometry. The percentages of annexin V/PI-positive cells are shown in the bar charts. (E) Reh cells were exposed to 10 μM Oba01 for 2 days. Then, caspase-3 and caspase-8 activation levels were analyzed by using a caspase-3 or caspase-8 activity assay kit. The p values were found to be two-tailed. **$p \leq 0.01$, ***$p \leq 0.001$, versus vehicle control.

indicating that the Oba01 could significantly and dose-dependently suppress the tumor growth in Reh mouse xenografts.

Next, anti-tumor efficacy of Oba01 was validated in two other subcutaneous xenograft models of ALL J. gamma1 and Jurkat E6-1 cells. BALB/c nude mice bearing the xenografts were given by a single intravenous injection of various dosages of Oba01, and the tumor sizes were observed for 21 days. As shown in Figures 4C, 4D, and S4B, Oba01 displayed an impressive and substantial anti-tumor activity in a dose-dependent manner. In the J.gamma1 model, 8 mg/kg Oba01 resulted in CR in 5 out of 10 animals. A significant tumoricidal activity was also observed in the 4 mg/kg group with a complete response in 50% of the mice bearing J.gamma1 xenografts (5 of 10). Moreover, in the Jurkat E6-1 model, 8 mg/kg Oba01 resulted in CR in 7 out of 8 animals. Additionally, tumoricidal activity was also observed in the 4 mg/kg group with a complete response in 37.5% of the mice bearing Jurkat E6-1 xenografts (three of eight), and 2 mg/kg Oba01 resulted in CR in one out of eight animals (Figures 4E, 4F, and S4C). However, in

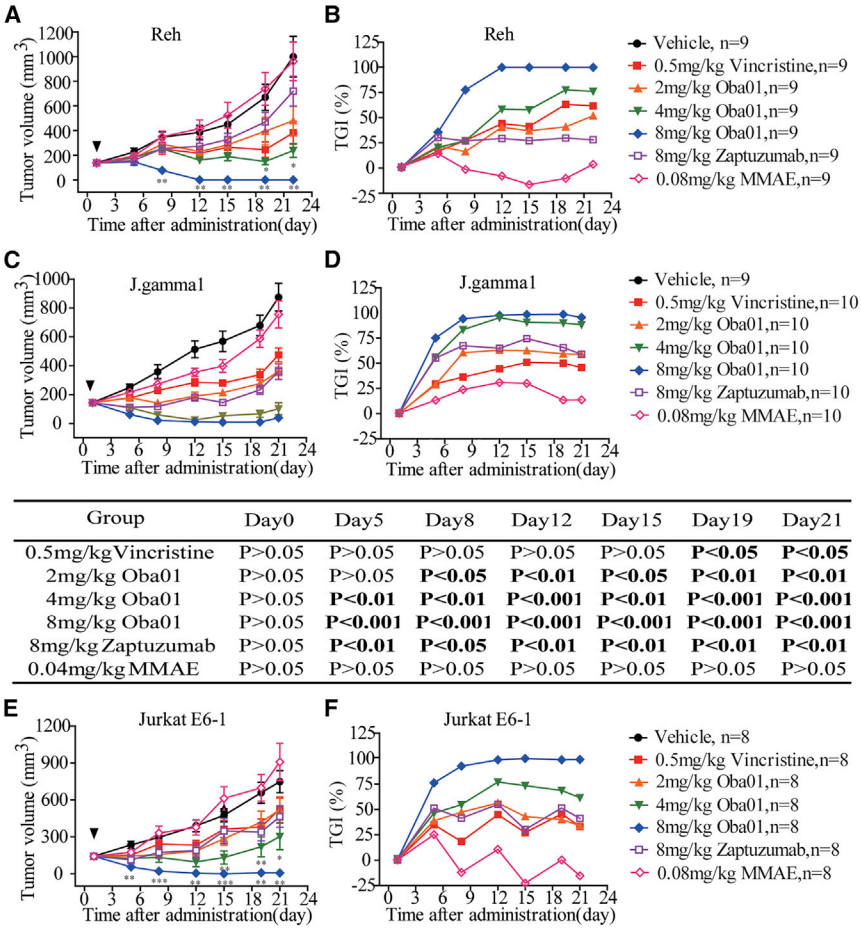

Group	Day0	Day5	Day8	Day12	Day15	Day19	Day21
0.5mg/kg Vincristine	P>0.05	P>0.05	P>0.05	P>0.05	P>0.05	**P<0.05**	**P<0.05**
2mg/kg Oba01	P>0.05	P>0.05	**P<0.05**	**P<0.01**	**P<0.05**	**P<0.01**	**P<0.01**
4mg/kg Oba01	P>0.05	**P<0.01**	**P<0.01**	**P<0.001**	**P<0.01**	**P<0.001**	**P<0.001**
8mg/kg Oba01	P>0.05	**P<0.001**	**P<0.001**	**P<0.001**	**P<0.001**	**P<0.001**	**P<0.001**
8mg/kg Zaptuzumab	P>0.05	**P<0.01**	**P<0.05**	**P<0.01**	**P<0.01**	**P<0.01**	**P<0.01**
0.04mg/kg MMAE	P>0.05	P>0.05	P>0.05	P>0.05	P>0.05	P>0.05	P>0.05

Figure 4. Antitumor activity of Oba01 in different sets of tumor models

(A–F) Transplanted tumor volumes were assessed in J.gamma1 (A and B), Reh (C and D), and Jurkat E6-1 (E and F) cells. BALB/c nude mice bearing xenografts (tumor size approximately averaged 150–200 mm^3) were intravenously (i.v.) injected with saline, 2.0, 4.0, and 8.0 mg/kg Oba01, or 0.5 mg/kg vincristine, 8.0 mg/kg zaptuzumab, or 0.08 mg/kg MMAE (the dose of MMAE equal to 4 mg/kg Oba01) once every 3 weeks. The dosing frequency is shown by arrowheads in the figures. The p values were found to be two-tailed. *$p \leq 0.05$, **$p \leq 0.01$, ***$p \leq 0.001$, versus vehicle control.

the two models, the free-form MMAE (0.08 mg/kg, an equal mole of MMAE in the dosage of 4 mg/kg Oba01) exhibited no substantial inhibitory effects, and the non-conjugated antibody zaptuzumab (8 mg/kg) also significantly suppressed the tumor growth. All of the treatment modalities did not lead to a notable change in the body weights of the mice (Figure S5). In addition, histopathological images of the mouse organ dissections clearly showed that Oba01 did not exhibit any notable adverse effects on the heart, liver, spleen, lung, and kidney (Figures S6–S8). Taken together, these data clearly demonstrate that Oba01 could significantly and dose-dependently exert an excellent and potent therapeutic efficacy in the different tumor xenograft mouse models of ALL.

To further confirm the efficacy of Oba01 in ALL mouse models, a T lymphocyte leukemia of the PDX model was established in non-obese diabetic (NOD)-severe combined immunodeficiency (SCID) mice by using HuKemia AL7174 patient lymphocyte leukemic cells. Thereafter, Oba01 was injected through the tail vein of mice (0 and 8 mg/kg, Q1W × 4). The results of this experiment demonstrated that the mice injected with 8.0 mg/kg of Oba01 survived for more than 71–74 days, but the mice that were administered with vehicle survived for 40–43 days after administration (Figure 5A). Moreover, the ratio of human $CD45^+$ cells to the live cells in the mouse peripheral blood as the mouse tumor burden index was detected weekly. The data demonstrated that the ratios of $CD45^+$ cells to the live mouse cells were significantly and rapidly decreased to almost zero after administration of Oab01 but not those of the vehicle control (Figure 5B). Importantly, there was no visible influence on the body weights in the animals treated with Oba01 (Figure 5C). These results further indicated that Oba01 could significantly suppress tumor growth in the ALL PDX model without exhibiting any side effects.

Safety evaluation in rats and cynomolgus monkeys

As mentioned above, all of the mice that were administered Oba01 in the mouse xenograft models appeared healthy and no notable body weight changes were observed. To further investigate the toxicity of Oba01 *in vivo*, in an acute toxicity study, a single dose of Oba01 (12, 24, and 48 mg/kg) and MMAE (0.46 mg/kg, an equal mole of MMAE in the dosage of Oba01 of 24 mg/kg) was intravenously injected into SD rats. As shown in Figure 6A, the maximal toxic dose (MTD) in SD rat was greater than 24 mg/kg, and the lethal dose was 48 mg/kg. However, the toxicity of Oba01 in SD rats was lower than that of the dose equivalent of MMAE alone. In addition, the acute toxicity study of Oba01 in cynomolgus monkeys was also conducted. A single dose of Oba01 (5, 10, and 20 mg/kg) and MMAE (0.19 mg/kg, an equal mole of MMAE in the dosage of Oba01 of 10 mg/kg) was intravenously administered into cynomolgus monkeys, respectively. As shown in Figure 6D, the MTD in cynomolgus monkeys was greater than 10 mg/kg, and the lethal dose was 20 mg/kg. Additionally, the toxicity of Oba01 in cynomolgus monkeys was lower than that of the dose equivalent of MMAE alone.

To further check the toxicity of Oba01 *in vivo*, a multiple-dosage toxicity study was performed in SD rats and cynomolgus monkeys. As shown in Figure 6B and Table S4, the MTD was more than 12 mg/kg, and the lethal dose was 36 mg/kg in SD rats, and there

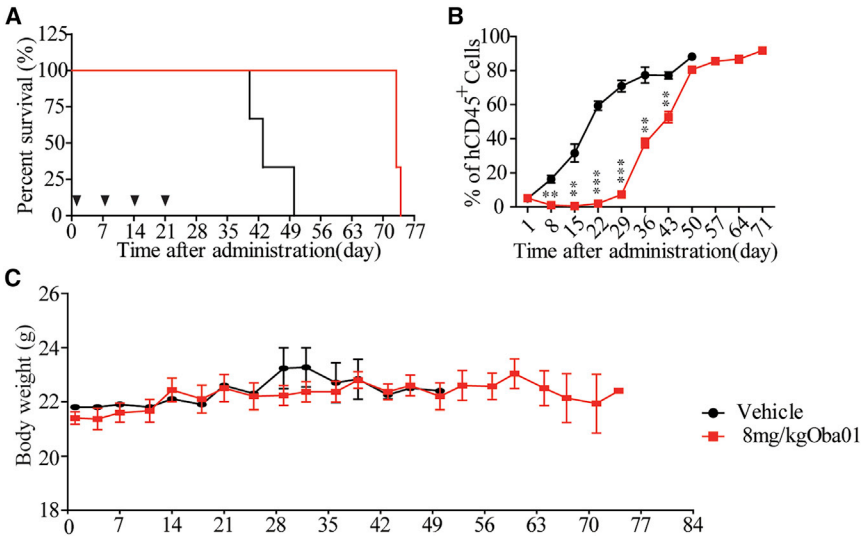

Figure 5. *In vivo* anti-tumor activity of Oba01 in acute lymphocyte leukemia PDX model AL7174

(A) Survival rate of AL7174 mice. (B) Tumor burden of AL7174 mice. (C) Body weight of AL7174 mice. The dosing frequency is shown by arrowheads in the figures. The p values were found to be two-tailed. **p ≤ 0.01, ***p ≤ 0.001, versus vehicle control.

were no Oba01-related effects on body weight. In the 36 mg/kg Oba01 group, the animals showed some toxic reactions, such as wasting, arching back, sparse coat, swelling, pallor, scab, tissue defect, and fluffy coat, and alanine aminotransferase (ALT), aspartate aminotransferase (AST), alkaline phosphatase (ALP), gamma-glutamyl transferase (GGT), cholesterol (CHO), creatine kinase (CK), and lactate dehydrogenase (LDH) were elevated (Table S6). Additionally, in the 0.23 mg/kg MMAE group, the body weight and food intake decreased. The toxicity of Oba01 of 12 mg/kg in SD rats was lower than that of the dose equivalent of MMAE alone. In addition, the MTD was more than 5 mg/kg and the lethal dose was 15 mg/kg in cynomolgus monkeys as shown in Figure 6E and Table S5, and there were no obvious abnormal changes in body weight in each dose group. In the 15 mg/kg Oba01 group, ALT, AST, CHO, CK, and LDH were elevated (Tables S7 and S8). Also, the toxicity of Oba01 of 5 mg/kg in cynomolgus monkeys was lower than that of the dose equivalent of MMAE alone. Therefore, a multiple-dose toxicity study of Oba01 in rats and cynomolgus monkeys showed excellent safety and tolerability *in vivo*.

Pharmacokinetics in rats and cynomolgus monkeys

The quantitation of total antibody, Oba01, and free-form MMAE was carried out in SD rat serum following a single-dose administration of 10 mg/kg (Figure 6C; Table S9) and in the serum of cynomolgus monkeys after a single-dose administration of 4 mg/kg (Figure 6F; Table S10). The pharmacokinetic parameters of Oba01 in SD rats and cynomolgus monkeys were basically the same as the total antibody, and area under the concentration-time curve (AUC) from time zero to the last quantifiable concentration (AUC_{last}), AUC from time zero to infinity (AUC_{inf}) were slightly lower than the total antibody, and half-time ($t_{1/2}$), mean residence time (MRT) elimination parameters of Oba01 were slightly different from the total antibody, and the elimination of Oba01 was slightly faster as compared to the total antibody. The content of MMAE in Oba01 was 1.9%, and the system exposure of MMAE in SD rats and cynomolgus monkeys was about 1:100,000 of Oba01, thereby indicating that Oba01 was substantially stable *in vivo* whereas the free form of MMAE was rapidly eliminated. Overall, the pharmacokinetic data clearly demonstrated that Oba01 was well tolerated in the rats and the monkeys with a favorable safety profile.

DISCUSSION

DR5 has been found to act as a potentially attractive therapeutic target for the development of anticancer agents, as it is exclusively expressed on the cell surface in various carcinomas, including lymphocytic leukemia, lung carcinoma, pancreatic cancer, colon cancer, breast cancer, ovarian cancer, and bladder cancer, among others, but with minimal expression in most normal cells.[6,21,23] DR5 can mediate apoptosis or autophagic cell death through initiating an intrinsic or extrinsic signaling pathway in tumor cells.[23,30] Anti-cancer therapies targeting DR5, including the use of recombinant soluble TRAIL (rsTRAIL) and anti-DR5 agonistic monoclonal antibodies, have been in clinical trials (phase I/II) for the treatment of multiple tumors.[24,25] We have also previously reported that the humanized anti-DR5 monoclonal antibody, zaptuzumab, has significant efficacy against lung carcinoma under *in vitro* and *in vivo* settings.

The concept of ADC has been well explored, and MMAE-based ADCs (such as brentuximab vedotin, polatuzumab vedotin, and enfortumab vedotin) are especially found to play an important role as anti-cancer therapeutics in the ADC arena.[10] Thus, exploiting molecular targets such as a DR5-targeting ADC can serve as a useful pharmacological strategy for developing therapeutics to improve antitumor activity in various malignancies. We have recently reported that Zapadcine-1 ADC using MMAD as payload could display an excellent antitumor activity against both solid tumor and hematological malignancies, but the therapeutic window was found to be relatively lower for its application in human cancer;[26] however, at present, no ADC using MMAD has been reported to enter the clinical development stage. This suggests that MMAE-based Oba01 ADC targeting DR5 may offer different clinical opportunities once tested in cancer patients.

In this study, we evaluated the functional characterization and potential antitumor activities of Oba01 on ALL cell lines *in vitro* and *in vivo*. We showed using FCM assays with Oba01 that DR5 was highly expressed on the cell surface of most lymphoblastic leukemia cell lines. It has been reported that immunohistochemistry (IHC) analysis of anti-DR5 (AD5-10) demonstrated that DR5 was highly expressed

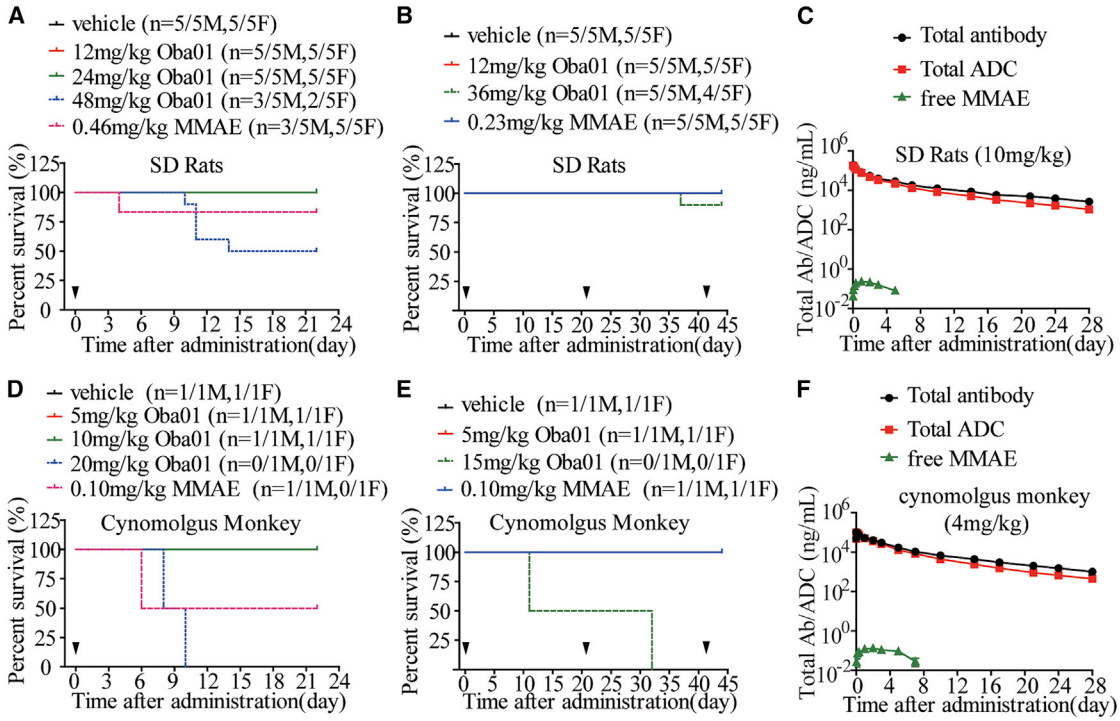

Figure 6. Preclinical safety and pharmacokinetics studies of Oba01 *in vivo*

(A and D) An acute toxicity study was performed after single dosing intravenously, and survival rates in SD rats (A) and cynomolgus monkeys (D) were analyzed. (B and E) A long toxicity study was performed after multiple dosing intravenously, and survival rates in SD rats (B) and cynomolgus monkeys (E) were analyzed. (C) Quantitation of total antibody, Oba01, and free MMAE was carried out in the serum from SD rats treated with a single intravenous administration of 10 mg/kg Oba01. (F) Quantitation of total antibody, Oba01, and free MMAE was carried out in the serum from cynomolgus monkeys treated with a single intravenous administration of 4 mg/kg Oba01. The dosing frequency is shown by arrowheads in the figures.

on the tissue arrays of most blood malignancies.[22] We observed that Oba01 selectively and significantly inhibited the proliferation of DR5-positive human lymphocyte leukemia cells, but not that of DR5-negative tumor cells. In contrast to Oba01, MMAE was found to be cytotoxic against all of the cell lines tested and did not discriminate between DR5-positive and DR5-negative cells. The results from the apoptosis analysis in Reh and TF-1 cells demonstrated that Oba01 could induce significant apoptosis in DR5-positive lymphocyte leukemia cells. Furthermore, it has been reported that the delivery of toxin payloads by cytotoxic antibodies is limited via efficient internalization of the antigen-ADC complex.[31] We noted that Oba01 could effectively bind to DR5 on the tumor cells and enter into the lysosomes via DR5-mediated endocytosis, where it releases the small molecule toxin MMAE from Oba01 by the degradation of proteases, which can then bind to the tubulin proteins to prevent tubulin aggregation, thus leading to a substantial inhibition of tumor cell proliferation and eventually resulting in tumor cell death. The findings further indicated that Oba01 displayed a high selectivity and specificity toward DR5-positive tumor cells.

Furthermore, the antitumor activity of Oba01 was evaluated in human acute lymphocyte leukemia xenograft mouse models. It was observed that Oba01 effectively eliminated the tumors and prevented recurrence, especially in the 4.0 and 8.0 mg/kg groups, and it even cleaned up tumors in Reh, J.gamma1, and Jurkat E6-1 CDX models, thereby displaying a significant dose-dependent efficacy and potent anti-tumor activity in tumor-baring mice. In contrast, free-form MMAE (0.08 mg/kg, an equivalent MMAE content to Oba01 of 4 mg/kg) displayed no significant inhibitory effect on tumor growth. However, zaptuzumab antibody alone (8 mg/kg) as a single agent suppressed tumor growth in this model but had a limited therapeutic effect comparable to the Oba01 at a dose of 2 mg/kg, thus indicating that Oba01 could significantly suppress the tumor growth in a dose-dependent manner. We also showed that Oba01 could significantly inhibit tumor growth in an ALL PDX model.

There have been several therapeutic anti-DR5 antibodies in clinical trials (phase I/II); however, Camidge et al.[32] reported that drozitumab monotherapy failed to show objective response in the patients with advanced solid tumors. It was also reported that the combination of conatumumab with carboplatin and paclitaxel for the treatment of non-small cell lung cancer (NSCLC), with panitumumab for metastatic colorectal cancer, or with doxorubicin for unrespectable soft tissue sarcoma were found to be not effective despite being well tolerated.[33] The main reason for this inefficacy may be that the complex mechanism of DR5-mediated signaling pathways might produce an

anti-apoptotic effect downstream of DR5 signaling. Thus, it is important that the DR5 targeting ADC cytotoxicity primarily depends on DR5 expressed on the cell membrane, rather than the intracellular DR5-mediated signaling cascades. Additionally, the anti-DR5 antibody can specifically and effectively target tumors, and this tumor-targeting capability exerts an important role for the distribution of toxin payload to kill the tumor cells. Therefore, Oba01 ADC not only retains high tumor specificity, comparable DR5 affinity, and excellent therapeutic efficacy, but it also avoids the complex intracellular signal transduction network, which might produce a sustained anti-apoptotic effect produced by using naked anti-DR5 antibody alone.

Moreover, compared to Zapadcine-1 ADC, Oba01 demonstrated a better safety profile in the acute toxicity study in both rats and cynomolgus monkeys. Preliminary safety evaluation demonstrated that the MTD of Oba01 in SD rats was found to be more than 24 mg/kg, and the lethal dose was 48 mg/kg. The MTD of Oba01 in cynomolgus monkeys was more than 10 mg/kg, and the lethal dose was 20 mg/kg. Additionally, in single-dose toxicity of MMAE in SD rats and cynomolgus monkeys, the toxicity of Oba01 was found to be significantly lower than that of the dose-equivalent MMAE alone. The therapeutic dosages in the mouse CDX model were as low as 2–8 mg/kg, which was approximately equal to less than 0.2–0.8 mg/kg in humans, thus indicating that the therapeutic window of Oba01 was excellent for human cancer therapy. Therefore, in contrast to Zapadcine-1, Oba01 could display significantly less toxicity and better safety in clinical studies.

Meanwhile, in the analysis of pharmacokinetic profiles of Oba01, total antibody and free MMAE were measured by ELISA and liquid chromatography-tandem mass spectrometry (LC-MS/MS), respectively. In SD rats and cynomolgus monkeys, the pharmacokinetic parameters of Oba01 were basically similar to those of the total antibody. AUC_{last} and AUC_{inf} were slightly lower than the total antibody, and $t_{1/2}$ MRT elimination parameters of Oba01 were slightly different from the total antibody. Finally, the conjugated MMAE concentrations decreased more rapidly than did the total antibody due to rapid antibody elimination and cytotoxic drug deconjugation.[34–36] Additionally, the level of free MMAE released from the ADC may be associated with significant loss of efficacy or even increased toxicity. Our data demonstrated that very low levels of free MMAE were detected for Oba01 in the systemic circulation, and the elimination of Oba01 *in vivo* was slightly faster than the total antibody. This reflected the potential stability of the linker and relatively limited deconjugation of MMAE from the conjugated zaptuzumab, which prevented induction of severe systemic toxicity. Therefore, we demonstrated that Oba01 could effectively release MMAE from Oba01 in the target tumor cells, and it was found to have favorable safety and pharmacokinetic profiles with excellent stability in both rats and cynomolgus monkeys.

Taken together, these preclinical findings demonstrate that Oba01 possesses a significant potential and dose-dependent tumoricidal activity in CDX and PDX mouse models, and a favorable safety profile, stability, and tolerability in SD rats and cynomolgus monkeys. Future studies are being planned to further demonstrate that Oba01 is an attractive and promising drug candidate for exploration in clinical settings in patients with DR5-positive lymphoblastic leukemia.

MATERIALS AND METHODS

Cell lines and animals

The human cell lines used in this study along with cell growth media are shown in Table S1. The identities of cell lines were validated by short tandem repeat (STR) DNA fingerprinting. The cells were cultured in RPMI 1640 medium (Gibco) supplemented with 10% fetal bovine serum (Gibco) and 1% penicillin/streptomycin (North China Pharmaceutical, Shijiazhuang, China) in a humidified incubator (Thermo Fisher Scientific, Waltham, MA, USA) with 5% CO_2 at 37°C.

BALB/c nude mice (5–6 weeks old) were purchased from GemPharmatech (Jiangsu, China). All animals were housed and maintained in a specific pathogen-free (SPF) grade of animal care facility. Five- to 6-week-old mice at initiation of the experiment were maintained with standard laboratory chow and water *ad libitum*. All animal experiments were approved and performed in full compliance with guidelines approved by the Animal Care Committee of the Center for Experimental Animals, Obio Technology (Shanghai, China).

Antibodies and Oba01 ADC

The fully humanized DR5-specific monoclonal antibody (zaptuzumab)[27,30] and its ADC (Oba01) were generated by Yantai Mabplex International Bio-Pharmaceutical (Shandong, China).[37] Oba01 was produced by enabling zaptuzumab coupled with a highly toxic inhibitor of tubulin, MMAE, via a proteinase cleavable linker by ThioBridge technology and formulated in 5 mM histidine, 175 mM trehalose, and 0.035% (w/v) Tween 20 (pH 6.0). The solution was filtered (0.22 μm) and stored at −80°C.[37]

Characterization of Oba01 was performed by size-exclusion chromatography (1200 series high-performance liquid chromatography [HPLC], Agilent Technologies, Wilmington, DE, USA) and hydrophobic interaction chromatography (HIC) as described by Hamblett et al.[37,38] The identification for peaks corresponding to ADCs with 2, 4, and 6 mol of toxin per mole of antibody was accomplished. The drug/Ab ratio was determined by peak area integration.

In vitro cytotoxicity assay

To determine *in vitro* anti-tumor activity, various lymphoblastic leukemia cell lines were treated with a 10-fold dilution series of ADC in triplicate in RPMI 1640 media supplemented with 10% heat-inactivated bovine serum (Gibco) for 3 days. Cell viability was measured with a CellTiter-Glo luminescent cell viability assay kit (Promega, G7572) according to the manufacturer's instructions, and absorbance was determined using a SPARK 10M multiplate reader (Tecan, Switzerland). Untreated cells served as controls. The cell survival rate (%) was calculated using the following formula: $(A_{sample}/A_{control}) \times 100\%$. The IC_{50}

was calculated using a non-linear regression analysis using GraphPad Prism 5.0.

Internalization assay

Reh lymphocyte leukemia cells were harvested and resuspended at a density of 1×10^6/mL in RPMI 1640 medium. 2.0 μg/mL Oba01 was thereafter incubated with the cells at 4°C for 1 h, and the cells were washed with RPMI 1640 medium. Then, the cells were incubated at 37°C for the indicated time intervals. Thereafter, the cells were washed three times in ice-cold RPMI 1640 medium and fixed with 4% paraformaldehyde for 10 min. The cells were then incubated with 1 μg/mL goat anti-human IgG (H+L) cross-adsorbed secondary antibody labeled with Alexa Fluor 488 (Invitrogen) at 4°C for 1 h, and thereafter washed twice with FCM buffer (PBS + 1% BSA) and resuspended in the ice-cold FCM buffer. The cell membrane staining was analyzed with a FCM Calibur (ACEA, NovoCyte 2060R, USA).

To examine Oba01 internalization and trafficking to the lysosome, approximately 1×10^6 Reh cells in the logarithmic growth phase were added on the Lab-Tek chambered cover glass (Thermo Fisher Scientific, Waltham, MA, USA). The cells were then incubated the next day with 2.0 μg/mL Oba01 at 4°C for 1 h, and thereafter the cells were washed twice with ice-cold RPMI 1640 medium and incubated at 37°C for the indicated time intervals followed by washing twice with ice-cold RPMI 1640 medium. The cells were then fixed with 4% paraformaldehyde and permeabilized with 0.05% Tween 20 in PBS for 10 min at 4°C. The cells on the cover glass were washed twice with ice-cold RPMI 1640 medium and incubated with 1 μg/mL LAMP1 (D2D11) XP rabbit monoclonal antibody (mAb) at 4°C for 1 h. The cells were washed twice with ice-cold RPMI 1640 medium and then incubated with 1 μg/mL goat anti-human IgG (H+L) cross-adsorbed secondary antibody labeled with Alexa Fluor 488 (green) (Invitrogen) and goat anti-rabbit IgG (H+L) highly cross-adsorbed secondary antibody labeled with Alexa Fluor 568 (red) at 4°C for 1 h. The nuclei were then counterstained with Hoechst 33342, washed twice with PBS, and covered with the coverslip. Images were captured by using a laser scanning confocal microscope (SP8, Leica, Germany).

Cell apoptosis

To evaluate apoptosis of Reh lymphocyte leukemia cells treated with Oba01, the cells were seeded at a density of 2×10^5 cells/well and exposed to Oba01 with various concentrations (0, 10, 30, and 100 μg/mL) for 48 h. The cells treated with medium alone were used as controls. Cell death was detected by using an annexin V-fluorescein isothiocyanate (FITC)/PI apoptosis kit (Beyotime Biotechnology, Shanghai, China) and measured by a FCM Calibur (Beckman, CytoFLEX LX, USA). Caspase-3 or caspase-8 activity was then determined by using caspase-3/8 activity assay kits (Beyotime Biotechnology, Shanghai, China) and measured by a microplate reader (SpectraMax M5, Molecular Devices, USA).

In vivo therapeutic efficacy analysis in ALL CDX models

1×10^7 Reh, J.gamma1, or Jurkat E6-1 cells suspended in 200 μL of PBS were injected subcutaneously into the right flank of BALB/c nude mice. When the tumor volume reached 100–200 mm^3, the mice were randomized into four or seven groups and injected intravenously with Oba01 at various doses at Q3D × 3, Q1W × 4, Q2W × 2, and Q3W × 1, respectively. Physiological saline was administered as a vehicle control. The tumor sizes were measured twice a week with calipers, and tumor volumes were determined according to the formula: tumor volume (mm^3) = (length × width^2) × 0.5. T/C was calculated as (treated tumor volume/control tumor volume) × 100%. The inhibition rate of the tumor growth (TGI) was calculated as (1 − treated tumor volume/control tumor volume) × 100%.

In vivo anti-tumor activity in ALL PDX model

To establish the T lymphocyte leukemia PDX model, HuKemia AL7174 cells (Crown Bioscience, Beijing, China) were thawed out from liquid nitrogen in a 37°C water bath rapidly and transferred into a 50-mL Falcon tube containing 40 mL of pre-warmed RPMI 1640 medium. The cells were pelleted by centrifugation at 1,000 rpm for 7 min, washed twice with ice-cold PBS, and then re-suspended into ice-cold PBS. The cells at a density of 2×10^6 were intravenously injected into NOD-SCID mice for tumor development, denoted as day 0. After inoculation, eye blood was collected weekly from the animals, and the human $CD45^+$ cells in the mouse peripheral blood mononuclear cells (PBMCs) were stained and determined by fluorescence-activated cell sorting (FACS) to monitor the tumor burden. When the average of the tumor burden reached about 5%, the mice were randomly divided into two different groups (n = 3). The day of grouping was denoted as day 1. The mice were intravenously injected with vehicle and 8 mg/kg Oba01 at days 1, 7, 14, and 21, respectively. Physiological saline was administered as the vehicle control. The tumor burden of each group was determined and analyzed accordingly. In addition, animals were monitored daily for vital signs, including weight, mobility, activity, appetite, appearance and grooming, hydration, color of limbs, and color of mucosa, among others.

Preclinical safety and pharmacokinetic studies

GLP (good laboratory practice) studies were conducted by JOINN Laboratories (Suzhou, China) in compliance with the animal welfare policies and guidelines approved by the National Medical Products Administration (NMPA) of China, including the toxicity study and pharmacokinetic study. The detailed methods are provided in the Supplemental materials and methods.

Statistical analysis

Results of all experiments are presented as mean values ± standard deviation (SD) by GraphPad Prism 5 software. IC_{50} values were determined by nonlinear regression analysis of concentration response curves using SPSS 16.0. The statistical significance between two groups was determined using a two-way ANOVA followed by a Student's t test. For all tests, p values less than 0.05 were considered statistically significant.

SUPPLEMENTAL INFORMATION

Supplemental information can be found online at https://doi.org/10.1016/j.omto.2021.04.013.

ACKNOWLEDGMENTS

We thank Dr. Changjiang Huang and his team of scientists at Yantai Mabplex International Bio-Pharmaceutical Co. Ltd. for technical and administrative support and valuable discussions regarding the design and manufacturing of zaptuzumab and Oba01. We gratefully acknowledge the technical support provided by scientists at JOINN Inc. for the preclinical safety and pharmacokinetic studies of Oba01. This project was supported by grants from State Key Project for Novel Drug Development, Ministry of Science and Technology of China (no. 2019ZX09732002-008-001), Shanghai Academic/Technology Research Leader, Shanghai Commission of Science and Technology (no. 18XD1420200), and by Shanghai Science and Technology Innovation Action Plan Supported Project in Biomedicine, Shanghai Commission of Science and Technology (no. 18431903100).

AUTHOR CONTRIBUTIONS

S.Z. designed the study, planned the experiments, analyzed and interpreted the data, and wrote and edited the manuscript. W.Z., C.Z., P.X., and D.Z. made efforts on acquisition of data, development of methodology, interpretation of data, and carrying out all of the experiments. D.Z. conceived the project and reviewed and edited the manuscript. All authors contributed to and approved the final manuscript.

DECLARATION OF INTERESTS

The authors declare no competing interests.

REFERENCES

1. Larson, R.A. (2006). Management of acute lymphoblastic leukemia in older patients. Semin. Hematol. *43*, 126–133.
2. Izraeli, S. (2010). Application of genomics for risk stratification of childhood acute lymphoblastic leukaemia: From bench to bedside? Br. J. Haematol. *151*, 119–131.
3. Advani, A.S. (2013). New immune strategies for the treatment of acute lymphoblastic leukemia: Antibodies and chimeric antigen receptors. Hematology (Am. Soc. Hematol. Educ. Program) *2013*, 131–137.
4. Roberts, K.G., and Mullighan, C.G. (2015). Genomics in acute lymphoblastic leukaemia: Insights and treatment implications. Nat. Rev. Clin. Oncol. *12*, 344–357.
5. Terwilliger, T., and Abdul-Hay, M. (2017). Acute lymphoblastic leukemia: A comprehensive review and 2017 update. Blood Cancer J. *7*, e577.
6. Wei, G., Wang, J., Huang, H., and Zhao, Y. (2017). Novel immunotherapies for adult patients with B-lineage acute lymphoblastic leukemia. J. Hematol. Oncol. *10*, 150.
7. Sievers, E.L., and Senter, P.D. (2013). Antibody-drug conjugates in cancer therapy. Annu. Rev. Med. *64*, 15–29.
8. Beck, A., Goetsch, L., Dumontet, C., and Corvaïa, N. (2017). Strategies and challenges for the next generation of antibody-drug conjugates. Nat. Rev. Drug Discov. *16*, 315–337.
9. Lambert, J.M., and Morris, C.Q. (2017). Antibody-drug conjugates (ADCs) for personalized treatment of solid tumors: A review. Adv. Ther. *34*, 1015–1035.
10. Joubert, N., Beck, A., Dumontet, C., and Denevault-Sabourin, C. (2020). Antibody-drug conjugates: The last decade. Pharmaceuticals (Basel) *13*, 245.
11. Drago, J.Z., Modi, S., and Chandarlapaty, S. (2021). Unlocking the potential of antibody-drug conjugates for cancer therapy. Nat. Rev. Clin. Oncol. Published online February 8, 2021. https://doi.org/10.1038/s41571-021-00470-8.
12. Jen, E.Y., Ko, C.W., Lee, J.E., Del Valle, P.L., Aydanian, A., Jewell, C., Norsworthy, K.J., Przepiorka, D., Nie, L., Liu, J., et al. (2018). FDA approval: Gemtuzumab ozogamicin for the treatment of adults with newly diagnosed CD33-positive acute myeloid leukemia. Clin. Cancer Res. *24*, 3242–3246.
13. Richardson, N.C., Kasamon, Y.L., Chen, H., de Claro, R.A., Ye, J., Blumenthal, G.M., Farrell, A.T., and Pazdur, R. (2019). FDA approval summary: Brentuximab vedotin in first-line treatment of peripheral T-cell lymphoma. Oncologist *24*, e180–e187.
14. Wedam, S., Fashoyin-Aje, L., Gao, X., Bloomquist, E., Tang, S., Sridhara, R., Goldberg, K.B., King-Kallimanis, B.L., Theoret, M.R., Ibrahim, A., et al. (2020). FDA approval summary: Ado-trastuzumab emtansine for the adjuvant treatment of HER2-positive early breast cancer. Clin. Cancer Res. *26*, 4180–4185.
15. Lamb, Y.N. (2017). Inotuzumab ozogamicin: First global approval. Drugs *77*, 1603–1610.
16. Deeks, E.D. (2019). Polatuzumab vedotin: First global approval. Drugs *79*, 1467–1475.
17. Keam, S.J. (2020). Trastuzumab deruxtecan: First approval. Drugs *80*, 501–508.
18. Hanna, K.S. (2020). Enfortumab vedotin to treat urothelial carcinoma. Drugs Today (Barc) *56*, 329–335.
19. Marsters, S.A., Sheridan, J.P., Pitti, R.M., Huang, A., Skubatch, M., Baldwin, D., Yuan, J., Gurney, A., Goddard, A.D., Godowski, P., and Ashkenazi, A. (1997). A novel receptor for Apo2L/TRAIL contains a truncated death domain. Curr. Biol. *7*, 1003–1006.
20. Walczak, H., Degli-Esposti, M.A., Johnson, R.S., Smolak, P.J., Waugh, J.Y., Boiani, N., Timour, M.S., Gerhart, M.J., Schooley, K.A., Smith, C.A., et al. (1997). TRAIL-R2: a novel apoptosis-mediating receptor for TRAIL. EMBO J. *16*, 5386–5397.
21. Daniels, R.A., Turley, H., Kimberley, F.C., Liu, X.S., Mongkolsapaya, J., Ch'En, P., Xu, X.N., Jin, B.Q., Pezzella, F., and Screaton, G.R. (2005). Expression of TRAIL and TRAIL receptors in normal and malignant tissues. Cell Res. *15*, 430–438.
22. Ramos-Medina, R., Montes-Moreno, S., Maestre, L., Cañamero, M., Rodriguez-Pinilla, M., Lázaro, A., and Roncador, G. (2011). Immunohistochemical analysis of HLDA9 Workshop antibodies against cell-surface molecules in reactive and neoplastic lymphoid tissues. Immunol. Lett. *134*, 150–156.
23. Naoum, G.E., Buchsbaum, D.J., Tawadros, F., Farooqi, A., and Arafat, W.O. (2017). Journey of TRAIL from bench to bedside and its potential role in immuno-oncology. Oncol. Rev. *11*, 332.
24. Lim, B., Greer, Y., Lipkowitz, S., and Takebe, N. (2019). Novel apoptosis-inducing agents for the treatment of cancer, a new arsenal in the toolbox. Cancers (Basel) *11*, 1087.
25. Dubuisson, A., and Micheau, O. (2017). Antibodies and derivatives targeting DR4 and DR5 for cancer therapy. Antibodies (Basel) *6*, 16.
26. Zhang, S., Zheng, C., Zhu, W., Xiong, P., Zhou, D., Huang, C., and Zheng, D. (2019). A novel anti-DR5 antibody-drug conjugate possesses a high-potential therapeutic efficacy for leukemia and solid tumors. Theranostics *9*, 5412–5423.
27. Chen, L., Qiu, Y., Hao, Z., Cai, J., Zhang, S., Liu, Y., and Zheng, D. (2017). A novel humanized anti-tumor necrosis factor-related apoptosis-inducing ligand-R2 monoclonal antibody induces apoptotic and autophagic cell death. IUBMB Life *69*, 735–744.
28. Abu-Qare, A.W., and Abou-Donia, M.B. (2001). Biomarkers of apoptosis: Release of cytochrome *c*, activation of caspase-3, induction of 8-hydroxy-2′-deoxyguanosine, increased 3-nitrotyrosine, and alteration of p53 gene. J. Toxicol. Environ. Health B Crit. Rev. *4*, 313–332.
29. Kong, A.N., Yu, R., Hebbar, V., Chen, C., Owuor, E., Hu, R., Ee, R., and Mandlekar, S. (2001). Signal transduction events elicited by cancer prevention compounds. Mutat. Res. *480-481*, 231–241.
30. Guo, Y., Chen, C., Zheng, Y., Zhang, J., Tao, X., Liu, S., Zheng, D., and Liu, Y. (2005). A novel anti-human DR5 monoclonal antibody with tumoricidal activity induces caspase-dependent and caspase-independent cell death. J. Biol. Chem. *280*, 41940–41952.
31. Chari, R.V., Miller, M.L., and Widdison, W.C. (2014). Antibody-drug conjugates: An emerging concept in cancer therapy. Angew. Chem. Int. Ed. Engl. *53*, 3796–3827.
32. Camidge, D.R., Herbst, R.S., Gordon, M.S., Eckhardt, S.G., Kurzrock, R., Durbin, B., Ing, J., Tohnya, T.M., Sager, J., Ashkenazi, A., et al. (2010). A phase I safety and pharmacokinetic study of the death receptor 5 agonistic antibody PRO95780 in patients with advanced malignancies. Clin. Cancer Res. *16*, 1256–1263.

33. Peeters, M., Price, T.J., Cervantes, A., Sobrero, A.F., Ducreux, M., Hotko, Y., André, T., Chan, E., Lordick, F., Punt, C.J., et al. (2010). Randomized phase III study of panitumumab with fluorouracil, leucovorin, and irinotecan (FOLFIRI) compared with FOLFIRI alone as second-line treatment in patients with metastatic colorectal cancer. J. Clin. Oncol. *28*, 4706–4713.

34. Kamath, A.V., and Iyer, S. (2015). Preclinical pharmacokinetic considerations for the development of antibody drug conjugates. Pharm. Res. *32*, 3470–3479.

35. Malik, P., Phipps, C., Edginton, A., and Blay, J. (2017). Pharmacokinetic considerations for antibody-drug conjugates against cancer. Pharm. Res. *34*, 2579–2595.

36. Zuo, P. (2020). Capturing the magic bullet: Pharmacokinetic principles and modeling of antibody-drug conjugates. AAPS J. *22*, 105.

37. Yao, X., Jiang, J., Wang, X., Huang, C., Li, D., Xie, K., Xu, Q., Li, H., Li, Z., Lou, L., and Fang, J. (2015). A novel humanized anti-HER2 antibody conjugated with MMAE exerts potent anti-tumor activity. Breast Cancer Res. Treat. *153*, 123–133.

38. Hamblett, K.J., Senter, P.D., Chace, D.F., Sun, M.M., Lenox, J., Cerveny, C.G., Kissler, K.M., Bernhardt, S.X., Kopcha, A.K., Zabinski, R.F., et al. (2004). Effects of drug loading on the antitumor activity of a monoclonal antibody drug conjugate. Clin. Cancer Res. *10*, 7063–7070.

OMTO, Volume *21*

Supplemental information

Preclinical evaluation of a novel antibody-drug conjugate targeting DR5 for lymphoblastic leukemia therapy

Shuyong Zhang, Dongdong Zhou, Chao Zheng, Peng Xiong, Wan Zhu, and Dexian Zheng

Supplementary Methods

In vitro binding assay by ELISA

High binding 96-well plates were coated with the recombinant DR5 extra-cellular domain (ECD) from mouse, SD rat, cynomolgus monkey and human (Sino Biological Inc., Beijing, China) and blocked with 0.05% Tween-20 containing 1 % BSA in PBS (PBST). Oba01 at varying concentrations were added and incubated at 37 °C for 1.0 h, then washed with PBST and incubated with HRP-labeled donkey anti-human IgG-H&L (Abcam, ab102438) at 37 °C for 1.0 h. The excess probe was washed with PBST. Then TMB (3,3',5,5'-Tetramethylbenzidine) substrate solution (Solarbio, Shanghai, China, PR1200) was added and incubated at room temperature for 5 to 10 min followed by adding stop solution (1.0 M H_2SO_4). The optical density at 450 nm was determined on SPARK 10M multiplate reader (TECAN, 1703004862, Switzerland).

Analysis of DR5 expression in various ALL cells by flow cytometry

DR5 expression in Jurkat E6-1, Jurkat, J.gamma1, Reh, A3, MT-4, TF-1, Kasumi-1 and Daudi cells was examined by flow cytometry following immunofluorescent staining. Briefly, cells (1×10^6 cells/tube) were incubated in duplicate in the presence of Oba01 (1 μg/mL) at 4°C for 30 min. Normal human IgG antibody was used as a negative control. After washing, the cells were stained with 1 μg/mL goat anti-Human IgG (H+L) cross-adsorbed secondary antibody labeled with Alexa Fluor 488 (Invitrogen) at 4°C for 1 h, and then washed twice with FCM buffer (PBS + 1% BSA). The fluorescent signals in individual samples were analyzed by flow cytometry using a FCM Calibur (ACEA, NovoCyte 2060R, USA).

Histopathology analysis

Samples were fixed overnight in 10% NBF and transferred to Dehydration machines. Paraffin embedding and cutting of tissue sections was performed by the Embedding Machine and LEICA Semi-Automated Rotary Microtome. For HE Staining on tissue Slides were baked 60 min at 60°C and were deparaffinized with

four rinses in xylene, hydrated using an alcohol gradient. Slides were then counterstained using hematoxylin and bluing reagents. Slides were then counterstained using eosin and dehydrated using an alcohol gradient. Slides were then cleared using xylene and sealed using medium. Imaging was done on a Leica Fluorescent Microscope.

Preclinical safety evaluation and pharmacokinetic assay

The GLP studies were performed at JOINN Laboratories, Inc. (Suzhou, China) in compliance with the animal welfare policies and guidelines approved by the National Medical Products Administration (NMPA) of China. Sprague-Dawley (SD) rats aged 6-8 weeks were purchased from Beijing Vital River Laboratory Animal Technology Co. (Beijing, China). Cynomolgus monkeys aged 3-5.5 years were purchased from Guangxi grandforest scientific primate Co. (Guangxi, China).

For acute toxicity study, SD rats and cynomolgus monkeys were randomized into four groups. SD rats were single-dosed intravenously on day 1 with vehicle, 12 mg/kg, 24 mg/kg and 48 mg/kg of Oba01, and 0.46 mg/kg MMAE (a dose equivalent to the dose administered as the Oba01 24 mg/kg), respectively (n = 5 male/5 female/group). Cynomolgus monkeys were single-dosed intravenously on days 1 with vehicle, 5 mg/kg, 10 mg/kg and 20 mg/kg of Oba01, and 0.19 mg/kg MMAE (a dose equivalent to the dose administered as the Oba01 10 mg/kg), respectively (n = 1 male/1 female/group). All animals were examined for mortality and clinical signs every day. Assessment of toxicity was based on mortality, clinical signs, food consumption, body weight, clinical and anatomic pathology. Necropsies were performed on Day 22 and tissues were routinely processed.

For multiple doses toxicity study, 40 SD rats and 8 cynomolgus monkeys (half males and half females) were randomly divided into four groups. Oba01 was intravenously administered once per 3 weeks for 6 weeks followed by a week treatment-free phase, with vehicle, 12 mg/kg and 36 mg/kg of Oba01, and 0.23 mg/kg MMAE (a dose equivalent to the dose administered as the Oba01 12 mg/kg) (n = 5

male and 5 female) in 40 SD rats and vehicle, 5 mg/kg and 15 mg/kg of Oba01, and 0.10 mg/kg MMAE (a dose equivalent to the dose administered as the Oba01 5 mg/kg) (n = 1 male and 1 female) in 8 cynomolgus monkeys. Various parameters, including clinical signs, and body weight were monitored. Two days after the last administration, all rats (half males and half females) from each group were sacrificed for gross and histopathological examination.

For pharmacokinetic (PK) analysis, six SD rats (3 male/3 female) in each group were administered single-dosed intravenously with Oba01 of 10 mg/kg. Blood samples were drawn prior to dosing on day 0, and at 5min, 1h, 4h, 8h, 24h, 48h, 72h, 120h (D6), 168h (D8), 240h (D11), 336h (D15), 408h (D18), 504h (D22), 576h (D25), 672h (D29) after dosing. Blood was collected from tail veins at specified time points, and serum was isolated and stored at -80 °C. Six cynomolgus monkeys (3 male/3 female) in each group were administered single-dosed i.v. infusion (20 min) with Oba01 of 4 mg/kg. Blood samples were drawn prior to dosing on day 0, and at 10min, 1h, 4h, 8h, 24h, 48h, 72h, 120h (D6), 168h (D8), 240h (D11), 336h (D15), 408h (D18), 504h (D22), 576h (D25), 672h (D29) after dosing. Blood was collected from vena cephalica antebrachii or vena saphena at specific time points, and serum was isolated and stored at -80 °C. Quantification of total antibody and ADC were determined by optimized ELISA. The determination of free MMAE was performed by liquid chromatography tandem mass spectrometry. The PK analysis was performed using the software WinNonlin (V6.4, Pharsight, Princeton, USA).

Supplementary Tables

Table S1. Source of cell lines and cell growth media

Cell Line	Source	Origin	Cell Growth Medium
Jurkat E6-1	Cell Bank of Chinese Academy of Shanghai Institutes for Biological Sciences (Shanghai, China)	T-cell acute lymphoblastic leukemia	RPMI 1640+10%FBS
Jurkat	Cell Bank of Chinese Academy of Shanghai Institutes for Biological Sciences (Shanghai, China)	T-cell acute lymphoblastic leukemia	RPMI 1640+10%FBS
J.gamma1	iCell Bioscience Inc. (Shanghai, China)	T-cell acute lymphoblastic leukemia	RPMI 1640+10%FBS
Reh	Cell Bank of Chinese Academy of Shanghai Institutes for Biological Sciences (Shanghai, China)	non T/B acute lymphoblastic leukemia	RPMI 1640+10%FBS
A3	iCell Bioscience Inc. (Shanghai, China)	Acute lymphoblastic leukemia	RPMI 1640+10%FBS
MT-4	iCell Bioscience Inc. (Shanghai, China)	T- Acute lymphoblastic leukemia	RPMI 1640+10%FBS +1% β-Mercaptoethanol
TF-1	iCell Bioscience Inc. (Shanghai, China)	Erythroid leukemia	RPMI 1640+10%FBS +1%GM-CSF
Kasumi-1	Cell Bank of Chinese Academy of Shanghai Institutes for Biological Sciences (Shanghai, China)	Acute Myeloid Leukemia	RPMI 1640+10%FBS
Daudi	Cell Bank of Chinese Academy of Shanghai Institutes for Biological Sciences (Shanghai, China)	Burkitt's lymphoma	RPMI 1640+10%FBS

Table S2. High molecular weight, low molecular weight and monomer designation by size exclusion chromatography showing area and percentage of each fraction occupying total area under curve at 280 nm, related to Figure 1.

Retention Time (min)	Designation	Area280nm(mAU*s)	% Area280nm
7.996	HMW Aggregates	64.01737	1.2496
9.273	Monomer	4972.25293	97.0538
10.027	LMW Fragment	86.92017	1.6966

Table S3. Individual DAR components as determined by Hydrophobic Interaction Chromatography showing percentage of each fraction occupying total area under curve at 280 nm, related to Figure 1.

Retention Time (min)	Designation	Area280nm(mAU*s)	% Area280nm
3.409	DAR1	75.43899	1.8986
4.336	DAR 2	302.80391	7.6206
5.42	DAR 3	1012.66406	25.4858
6.309	DAR 4	1473.97003	37.0954
7.149	DAR 5	791.88899	19.9295
7.963	DAR 6	316.45347	7.9701

Table S4. Body weight in SD rat, related to Figure 6.

Group	Sex	Day(s) Relative to Start Date			
		-1	7	14	21
Control	Male	220.8 ± 2.7	282.6 ± 2.9	335.2 ± 3.8	376.0 ± 6.4
	Female	205.8 ± 2.1	224.8 ± 2.7	242.2 ± 4.7	260.6 ± 7.4
Oba01 12 mg/kg	Male	221.6 ± 2.6	272.8 ± 5.7	322.4 ± 10.5	369.0 ± 14.4
	Female	205.8 ± 2.4	230.0 ± 2.1	240.4 ± 5.2	256.6 ± 5.2
Oba01 36mg/kg	Male	220.4 ± 2.1	245.6 ± 8.5	291.2 ± 11.0	350.0 ± 8.6
	Female	205.2 ± 3.0	209.4 ± 7.7	226.0 ± 12.3	252.6 ± 6.3
MMAE 0.23mg/kg	Male	222.6 ± 2.8	258.0 ± 3.4	312.0 ± 4.7	358.2 ± 7.0
	Female	205.2 ± 2.8	222.0 ± 3.5	241.6 ± 5.6	262.6 ± 8.8

Group	Sex	Day(s) Relative			
		28	35	42	44
Control	Male	404.6 ± 6.9	432.8 ± 7.1	454.4 ± 7.6	437.6 ± 8.0
	Female	271.4 ± 3.0	275.4 ± 4.0	272.8 ± 3.6	263.2 ± 3.4
Oba01 12mg/kg	Male	389.6 ± 16.1	422.4 ± 18.1	449.2 ± 19.8	431.8 ± 18.0
	Female	268.2 ± 8.3	278.8 ± 6.8	273.0 ± 7.3	261 ± 7.7
Oba01 36mg/kg	Male	360.6 ± 9.9	400.4 ± 10.3	435.4 ± 7.2	413.8 ± 5.9
	Female	251.2 ± 10.1	247.2 ± 22.9	275.0 ± 5.3	266.0 ± 5.1
MMAE 0.23mg/kg	Male	375.6 ± 7.9	409.2 ± 11.4	435.8 ± 12.9	427.0 ± 14.8
	Female	268.4 ± 9.2	283.0 ± 11.3	283.4 ± 10.0	279.4 ± 7.8

Table S5. Body weight in cynomolgus monkeys, related to Figure 6.

Group	Sex	Day(s) Relative									
		-2	7	11	14	21	28	32	35	42	44
Control	Male	4.06	4.12	-	4.10	4.08	4.20	-	4.14	4.06	4.08
	Female	2.54	2.46	-	2.50	2.52	2.54	-	2.58	2.56	2.56
Oba01 5mg/kg	Male	2.48	2.48	-	2.50	2.50	2.58	-	2.58	2.50	2.54
	Female	2.54	2.60	-	2.56	2.52	2.70	-	2.64	2.62	2.62
Oba01 15mg/kg	Male	2.84	2.88	2.72	-	-	-	-	-	-	-
	Female	2.80	2.74	-	2.70	2.68	2.68	2.54	-	-	-
MMAE 0.10mg/kg	Male	3.94	3.92	-	3.76	3.84	3.94	-	3.98	4.02	4.00
	Female	2.46	2.40	-	2.36	2.42	2.46	-	2.54	2.36	2.32

Table S6. Primary blood-chemistry parameters in SD rats

Group	Sex	ALT (U/L)	AST (U/L)	ALP (U/L)	GGT (U/L)	CK (U/L)	LDH (U/L)	CHO (mM)	TG (mM)
Ctl	male	73±8	190±47	167±31	0.4±0.5	426±167	817±362	1.99±0.24	0.54±0.12
	female	53±12	134±20	64±14	1±0	461±254	938±565	2.37±0.60	0.61±0.11
12 mg/kg	male	78±5	170±17	182±41	0.8±0.4	328±70	616±166	2.14±0.24	0.51±0.12
Oba01	female	60±4	147±16	68±14	0.8±0.4	430±163	943±380	2.43±0.69	0.47±0.15
36 mg/kg	male	103±11	293±57	257±67	3.4±2.2	812±426	1352±721	2.98±0.63	0.64±0.21
Oba01	female	211±145	564±377	114±35	4.5±5.5	942±318	1922±746	3.51±0.54	0.74±0.13
0.23 mg/kg	male	118±34	327±73	243±45	1.8±1.6	503±182	867±553	3.12±0.40	1.45±0.51
MMAE	female	96±15	273±17	75±18	1.2±0.4	492±77	713±170	2.67±0.44	1.85±0.55

Table S7. Primary blood-chemistry parameters in male cynomolgus monkeys

Group	Day	ALT (U/L)	AST (U/L)	ALP (U/L)	GGT (U/L)	CK (U/L)	LDH (U/L)	CHO (mM)	TG (mM)
0 mg/kg (Oba01)	-1	163	190	623	63	7560	1160	3.29	0.59
	8	140	48	676	53	286	542	3.25	0.93
	29	82	50	703	60	323	427	3.69	0.98
	43	62	46	635	60	286	363	3.98	0.60
	44	123	144	573	57	7145	1180	3.38	0.52
5 mg/kg (Oba01)	-1	71	47	435	59	362	539	3.81	0.45
	8	71	46	419	53	174	565	3.80	0.48
	29	81	45	463	59	227	508	4.11	0.50
	43	64	37	450	61	242	446	4.42	0.64
	44	63	57	382	54	422	516	3.53	0.45
15 mg/kg (Oba01)	-1	55	80	381	56	761	479	3.33	0.47
	8	62	152	398	61	1410	1602	5.17	0.34
	11	170	728	238	60	62000	6580	2.22	0.79
0.10 mg/kg (MMAE)	-1	86	88	739	96	396	494	2.51	0.37
	8	89	28	703	72	165	406	2.50	0.31
	29	49	23	759	71	154	374	2.47	0.35
	43	39	28	689	75	215	316	2.59	0.46
	44	79	130	641	73	3415	977	2.31	0.44

Table S8. Primary blood-chemistry parameters in female cynomolgus monkeys

Group	Day	ALT (U/L)	AST (U/L)	ALP (U/L)	GGT (U/L)	CK (U/L)	LDH (U/L)	CHO (mM)	TG (mM)
0 mg/kg (Oba01)	-1	35	62	372	78	236	387	2.68	0.57
	8	26	38	337	73	171	351	2.70	0.42
	29	28	38	345	85	209	331	2.80	0.39
	43	32	46	389	91	223	348	3.01	0.59
	44	35	44	367	93	284	428	3.07	0.36
5 mg/kg (Oba01)	-1	101	184	246	60	690	632	3.11	0.52
	8	112	73	299	50	352	473	3.87	0.57
	29	61	48	293	62	218	434	4.09	0.56
	43	39	36	283	56	235	327	3.72	0.45
	44	49	69	244	52	793	492	3.21	0.36
15 mg/kg (Oba01)	-1	201	335	403	61	1725	1320	1.92	0.58
	8	221	358	454	63	4020	2340	2.59	0.56
	29	48	102	553	61	245	969	1.89	0.38
0.10 mg/kg (MMAE)	-1	59	38	304	32	142	241	3.65	0.53
	8	70	31	223	26	149	252	3.16	0.53
	29	38	18	259	28	90	170	3.20	0.53
	43	40	19	221	29	89	171	3.63	0.56
	44	60	48	222	29	1148	395	3.51	0.69

Table S9. PK parameters in SD rats related to Figure 6.

Analyte		$t_{1/2}$ h	T_{max} h	C_{max} μg/mL	AUC_{last} h·mg/mL	AUC_{inf} h·mg/mL	MRT_{last} h
Total ADC	male	238	0.0833	209	9.63	10.0	108
	female	140	1.00	177	9.62	9.82	117
Total Ab	male	209	0.0833	222	12.0	12.8	135
	female	148	1.00	185	12.3	12.9	152
MMAE	male	66.6	24	0.237	19.6	28.6	52.4
	female	NA	48	0.233	20.4	NA	49.2

Table S10. PK parameters in cynomolgus monkey related to Figure 6.

Analyte		$t_{1/2}$ h	T_{max} h	C_{max} μg/mL	AUC_{last} h·mg/mL	AUC_{inf} h·mg/mL	MRT_{last} h
Total ADC	Mean	136	101	96.7	6.07	6.17	0.444
	SD	38.0	3.82	13.7	0.785	0.847	0.272
Total Ab	Mean	167	105	123	7.35	7.63	0.333
	SD	49.8	4.34	17.2	1.10	1.34	0.00
MMAE	Mean	115.4	0.13	68.29	14.75	25.80	40.00
	SD	42.68	0.03	11.33	2.86	3.54	12.39

Supplementary data

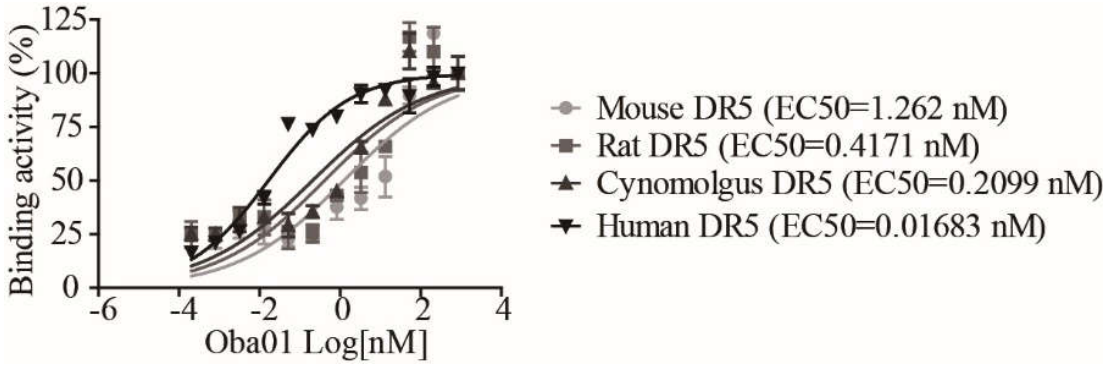

Figure S1. Binding activity of Oba01 to different species DR5. The binding activity of Oba01 in the recombinant mouse, SD rat, cynomolgus monkey and human DR5 antigen as estimated by ELISA.

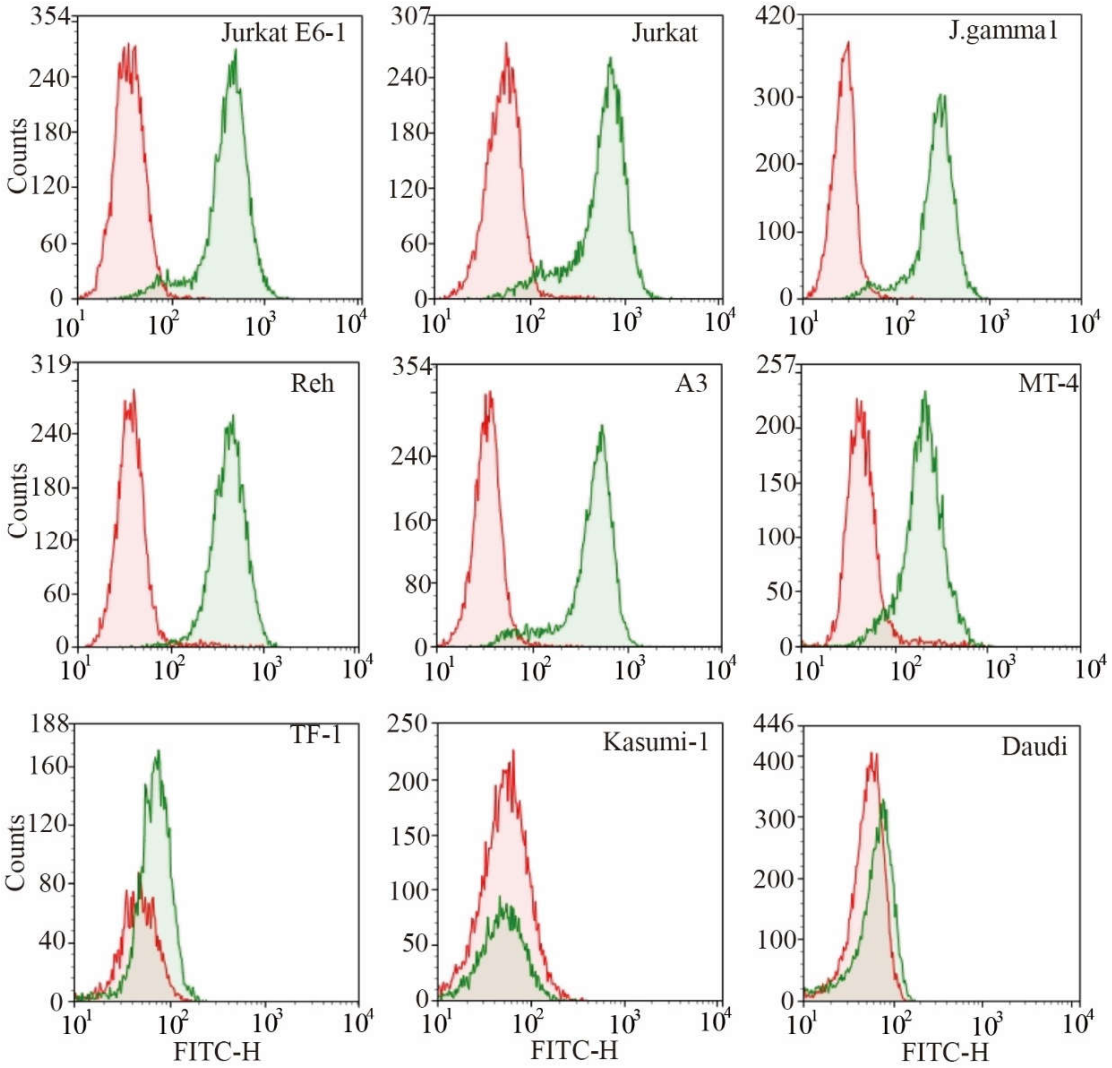

Figure S2. The binding specificity of Oba01 in the Jurkat E6-1, Jurkat, J.gamma1, Reh, A3, MT-4, TF-1, Kasumi-1 and Daudi cells. Anti-human IgG antibody was used as control and the cell-associated fluorescence was determined by FACS.

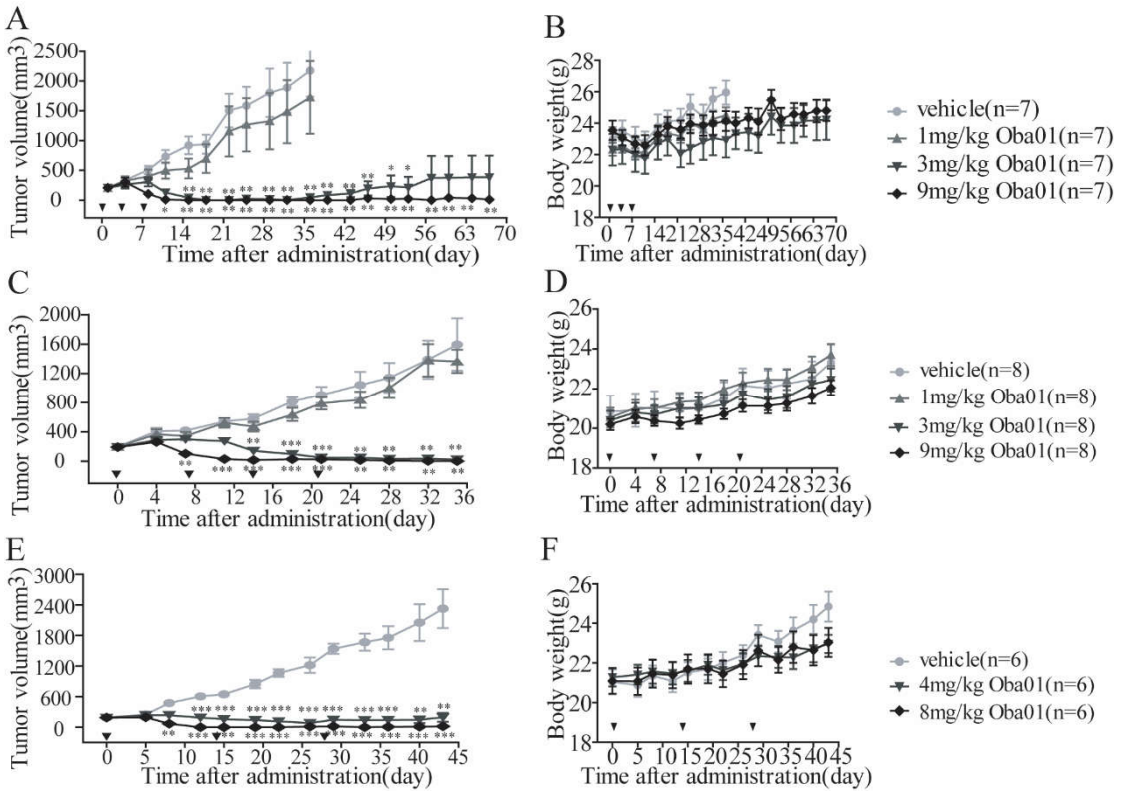

Figure S3. In vivo antitumor efficacy of Oba01 in subcutaneously implanted Reh xenograft model. The transplanted tumor volume and mouse body weights were assessed after administration. BALB/c nude mice bearing xenografts of human Reh lymphocyte leukemia were intravenously injected saline and Oba01 once every three days for 3 different times (Q3D×3) at 1, 3 and 9 mg/kg (A), once every week for 4 times (Q1W×4) at 1, 3 and 9 mg/kg (B), and once every two weeks for 3 times (Q2W×3) at 4 and 8 mg/kg (C), respectively. The dosing frequency has been shown by triangular arrowheads in the figures. The *p* values were found to be two-tailed, **p* ≤ 0.05, ***p* ≤ 0.01, ****p* ≤ 0.001. versus vehicle control.

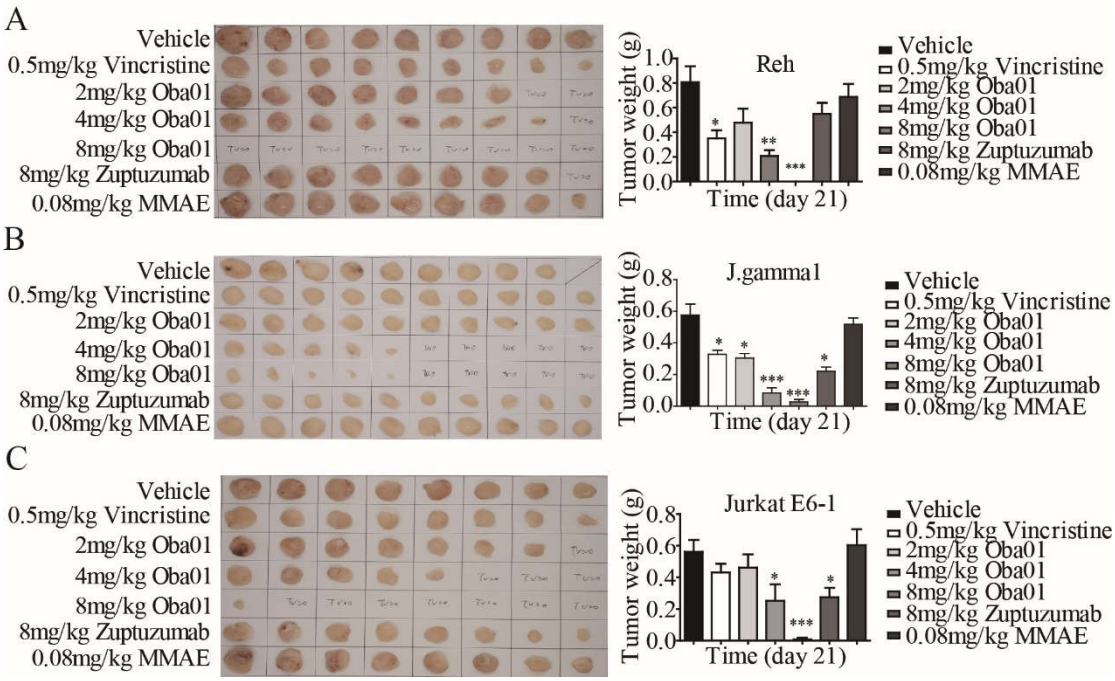

Figure S4. Efficacy of Oba01 in the mouse xenografts of human acute lymphocyte leukemia cells J.gamma1 (A), Reh (B) and Jurkat E6-1 (C), related to Figure 4 as indicated above. The representative transplanted tumor images and tumor weights were assessed at the end of the experiment. The *p* values were found to be two-tailed, $*p \leq 0.05$, $**p \leq 0.01$, $***p \leq 0.001$. versus vehicle control.

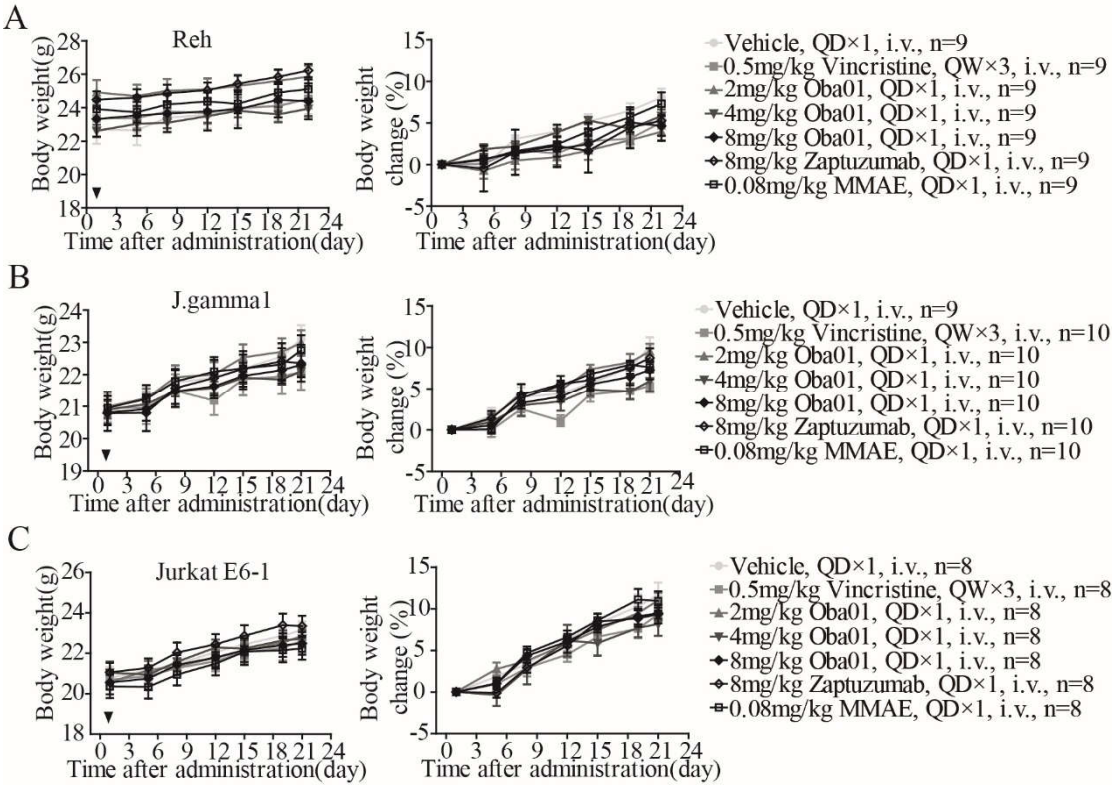

Figure S5. Efficacy of Oba01 in mouse xenografts of human acute lymphocyte leukemia cells Reh (A), J.gamma1 (B) and Jurkat E6-1 (C), related to Figure 4 as indicated above. Representative transplanted tumor mouse body weights and the changes of the body weights were assessed twice every week. The dosing frequency has been shown by triangular arrowheads in the figures.

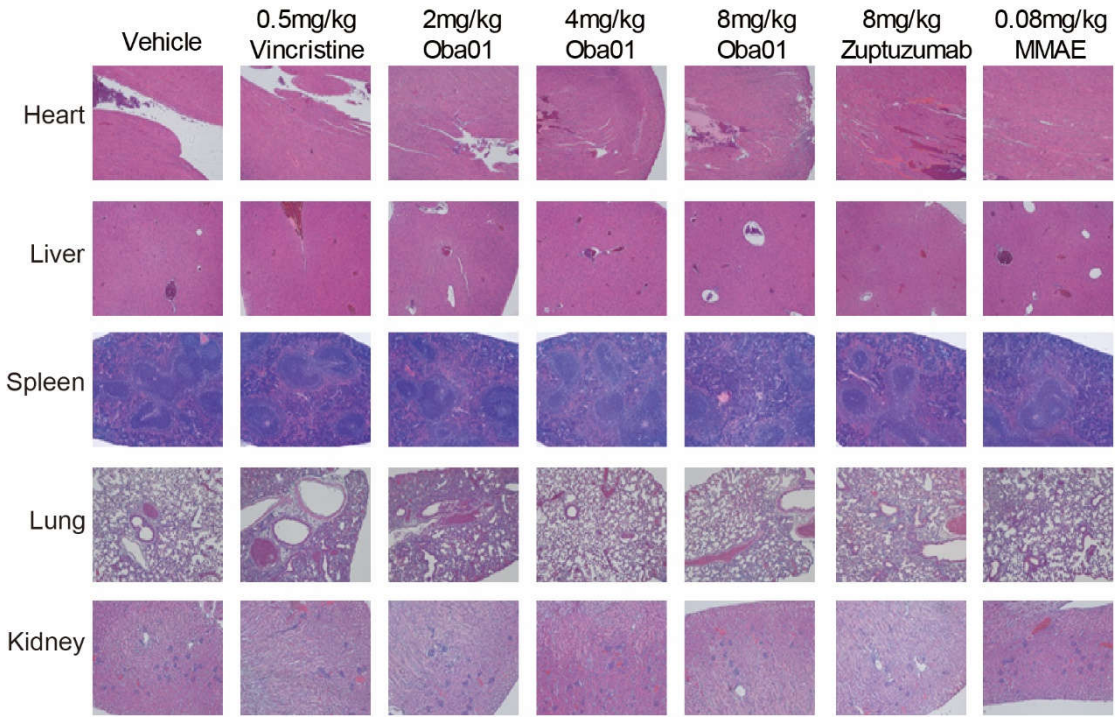

Figure S6. Oba01 had no effects on heart, liver, spleen, lung and kidney in human Reh mouse CDX models. H&E staining assay for the evaluation of pathological changes in these organs of human Reh mouse CDX models, related to Figure 4. Images captured at 40× magnification. Scale bars = 50 μm.

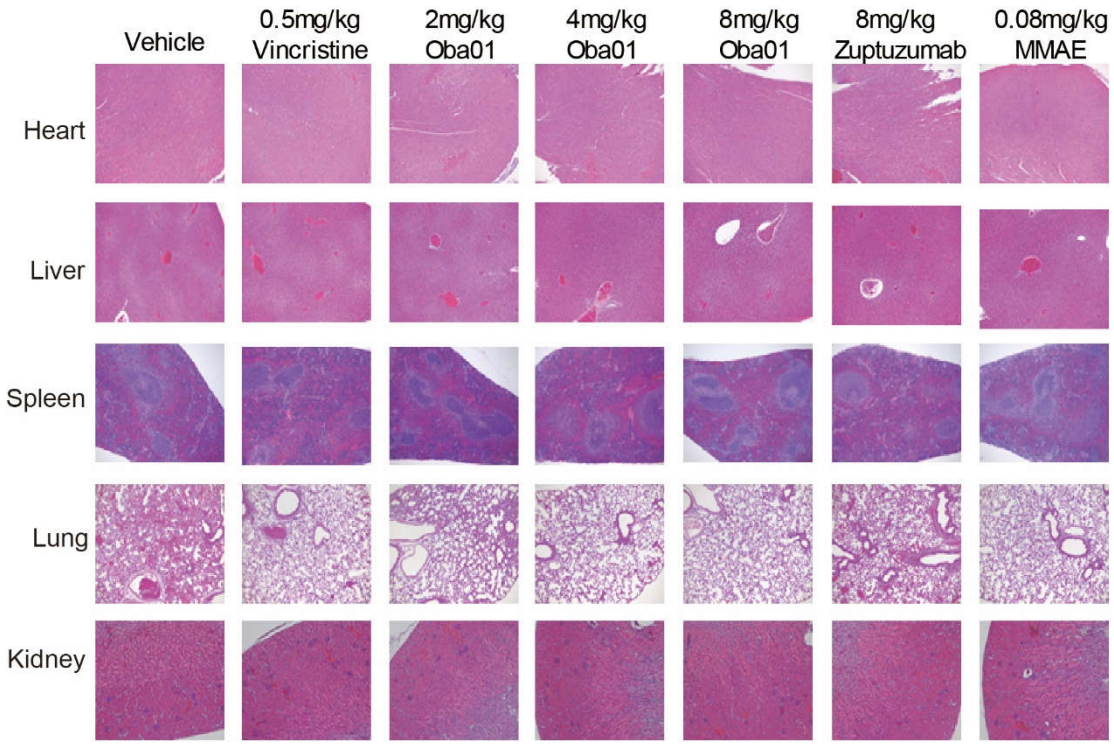

Figure S7. Oba01 had no effects on heart, liver, spleen, lung and kidney in human J.gammal mouse CDX models. H&E staining assay for the evaluation of pathological changes in these organs of human J.gammal mouse CDX models, related to Figure 4. Images captured at 40× magnification. Scale bars = 50 μm.

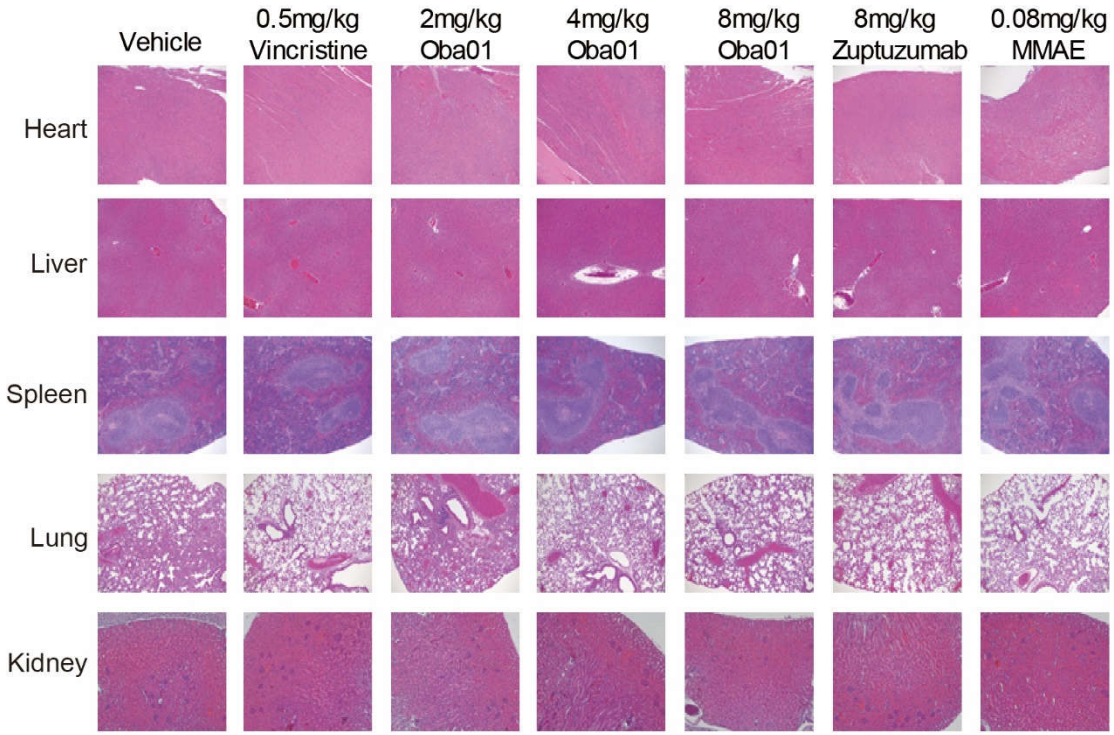

Figure S8. Oba01 had no effects on heart, liver, spleen, lung and kidney in human Jurkat E6-1 mouse CDX models. H&E staining assay for the evaluation of pathological changes in these organs of human Jurkat E6-1 mouse CDX models, related to Figure 4. Images captured at 40× magnification. Scale bars = 50 μm.